2017

A Study of the Correlation Between Static and Dynamic Modulus of Elasticity on Different Concrete Mixes

Logan Trifone

A STUDY OF THE CORRELATION BETWEEN STATIC AND DYNAMIC MODULUS OF ELASTICITY ON DIFFERENT CONCRETE MIXES

LOGAN TRIFONE

THESIS SUBMITTED TO THE

Benjamin M. Statler College of Engineering and Mineral Resources

at West Virginia University

IN PARTIAL FULFILLMENT OF THE REQUIREMENTS FOR THE DEGREE OF MASTERS OF SCIENCE

IN

CIVIL ENGINEERING

Roger H. L. Chen, Ph.D, Chair

P.V.Vijay, Ph.D

Yoojung Yoon, Ph.D

Department of Civil and Environmental Engineering

Morgantown, West Virginia

2017

Keywords: Dynamic Modulus of Elasticity, Static Modulus of Elasticity, Ultrasonic Pulse Velocity, Vibration Resonance Frequency

Abstract

This study is to determine the relationship between the Static Modulus of Elasticity and the Dynamic Modulus of Elasticity in various concrete mixes. The Static Loading Test was used to measure the strains associated with applied stresses on cylindrical concrete specimens to determine the Static Modulus. An Ultrasonic Pulse Wave Velocity (UPV) technique was utilized to measure the travel time of pulse waves propagating through rectangular prism specimens. The travel times were used to compute the Dynamic Modulus of Elasticity. An Impact Hammer measuring device was also used to measure resonance frequencies of vibrations in rectangular prisms, which also correlate to the Dynamic Modulus.

Four different concrete mixes were cast and each underwent the testing at 1, 3, 7, 14, and 28 days. The four concrete mixes were a 50% Slag mix, a 30% Flyash mix, an Ordinary Portland Cement (OPC) mix, and a Self-Consolidating Concrete (SCC) mix. The relationships between different calculated moduli values were plotted against each other to determine the correlation between them. Empirical relationships based on these values were then determined. The Static Modulus values were also computed using ACI 318 equations, and were compared to the measured Static Modulus values.

The results show that the Dynamic Modulus of Elasticity is higher than the Static Modulus of Elasticity for each concrete mix. The Dynamic Modulus obtained from UPV resulted in the highest values, while the Static Modulus was the lowest at all ages. The relationship between the Static and Dynamic Modulus is linear. The Dynamic Modulus from UPV and Vibration methods also exhibits a linear relationship. Empirical equations were developed to estimate the Modulus of Elasticity at different ages.

SCC had a much higher compressive strength compared to other concrete mixes. The use of ACI 318 equations to estimate Young's Modulus from 28-day compressive strength yielded conservative values as compared to the measured Static Modulus values.

Acknowledgement

I would like to thank my advisor, Dr. Roger Chen for his guidance, feedback, and provision throughout this study. I would also like to think my Thesis Committee, Dr. Yoojung Yoon, and Dr. P.V. Vijay for their time and effort. I would like to acknowledge WVDOT, whose funding provided the materials and equipment necessary to conduct this research. I would like to thank the entire research team, for assistance with all concrete castings necessary to complete this research study. I am very grateful to Guadalupe Leon, and Navid Mardmomen for assisting me with frequent concrete testing and setups in the lab.

I would like to thank my family for their constant support throughout my undergraduate and graduate career. I would not have gotten anywhere without them. Finally, I would like to thank my fiancé, Sarah, for her unsurmountable encouragement, and reassurance over the last several years. I am forever grateful.

Table of Contents

List of Figures

List of Tables

List of Equations

Chapter 1 Introduction

1.1 – Background

1.1.1 – Static and Dynamic Young's Modulus

The Modulus of Elasticity is also known as Young's Modulus, E, and is defined as "the ratio of the axial stress to axial strain for a material subjected to uni-axial load" (Popovics, 2008). Young's Modulus is one of the most important material properties of concrete, as it is always used throughout the structural design process. Building specifications often require a specific value of E to be met to ensure the structural integrity of the building is satisfactory, and to prevent unsatisfactory deformations. One example of this is Two Union Square Building located in Seattle, Washington. The designer of the building required that the Modulus of Elasticity of the concrete be at least 50 GPa (Popovics, 2008). Young's Modulus is always required to analyze the deflection of a structure. Concrete structural members must be designed appropriately to prevent lateral and longitudinal deformations, and to ensure that the applied loads do not exceed the capacity of the members.

Once concrete structures have been erected, the in situ properties can be difficult to determine without damaging the structure. Often, companion core samples are drilled out of the structure and loaded to failure to determine the compressive strength. There is an empirical relationship between the compressive strength and the modulus of elasticity of the concrete, however the formula provides overly conservative results. This can result in higher material costs by selecting concrete with a much higher strength than the required strength.

There are many different types of dynamic Non-Destructive testing (NDT) methods that can be used to estimate Young's Modulus of in situ structures. These include ultrasonic pulse velocity methods, resonance frequency methods, and other wave propagation techniques. The problem with the determination of this dynamic modulus, E_d, is that E_d is often found to be higher than that of the static modulus, E. The stress strain relationship of concrete can be complex due to the behavior of its gel structure and the manner in which water is held in concrete (Chavhan & Vyawahare, 2015). The Static Modulus is found by loading the concrete and measuring the slope of the stress-strain curve. Dynamic testing methods apply very little force as compared to the static loading. Dynamic testing methods will not result in any additional deformations of the concrete. This is regarded as the basis of why the dynamic modulus often proves to be higher than the Static Modulus.

As mentioned, there are several different non-destructive methods that can be used to compute E_d. The pulse wave propagations techniques and vibration resonance techniques are the most commonly used NDT methods used to determine E_d. It has been seen that the ultrasonic pulse velocity method results in higher E_d values than those obtained from vibration resonance methods. It should also be noted that the specimen shape can have an influence on the dynamic modulus value. Generally, prismatic beams undergoing vibration resonance produces a higher dynamic modulus than cylinders cast from the same concrete batch (Chavhan & Vyawahare, 2015).

The relationship between the Static Young's Modulus, and Dynamic Young's Modulus proves to be complex, and varies based on several factors. Concrete mixture, specimen size/shape and testing methods are all factors that influence the correlation between E_d and E.

1.1.2 – Non-Destructive Testing Techniques

As previously mentioned, E_d can be determined from a number of different dynamic based tests. Pulse wave propagation and vibration resonance methods are the two main NDT techniques used in the determination of E_d in concrete specimens. Each of these techniques will be utilized in this study. Computing the compressive strength of concrete and applying loads up to 35% of the strength to cylindrical concrete specimens is another widely-used NDT method to compute the static modulus, E. As technology advances, NDT and evaluation techniques are becoming more widespread and easier to use.

In addition to the determination of Young's Modulus, the utilization of these NDT techniques can also be used to determine concrete uniformity, voids, discontinuities, and other concrete properties. Non-destructive testing is commonly used in various industries and materials, such as steel, timber, and composite elements.

1.2 – Objectives and Scope

The goal of this research study is to develop empirical relationships between the Static Young's Modulus, E, and the Dynamic Young's Modulus, E_d for several different commonly used concrete mixes. Utilizing various dynamic Non-Destructive Testing techniques (Ultrasonic Pulse Velocity and Impact Resonance Frequency) is imperative to developing this relationship. In addition, a relationship between the E_d found from UPV, and E_d found from Impact Resonance frequency analysis is to be determined. Four different types of concrete mixes (Slag, Flyash, Ordinary Portland Cement, and Self-Consolidating Concrete) will be cast in-house to determine the above-mentioned properties. These empirical relationships will then be compared to similar

analysis conducted by various researchers to determine the accuracy and validity of the analysis. The compressive strength will be used to estimate Young's Modulus from ACI equations, and these values will be compared to the obtained values from the Static Modulus Test.

Chapter 2 Literature Review

2.1 – Static and Dynamic Modulus in Concrete

As previously mentioned, the Static Modulus of Elasticity and the Dynamic Modulus of Elasticity tend to differ. In one study conducted by John S. Popovics in 2008 from the University of Illinois, several empirical relationships were developed between the Static Modulus, E, and the Dynamic Modulus, E_d. Based on a large sample of concrete specimens, with compressive strengths ranging from 24MPa to 161MPa, he developed the following equation:

$$E = 0.83E_d$$

Equation 2-1 *– Relationship between E and E_d (Popovics, 2008).*

Popovics also produced a more detailed equation using the density of the concrete. This equation was said to be sufficient for both lightweight and normal weight concrete:

$$E = kE_d^{1.4}\rho^{-1}$$

Equation 2-2 *- Relationship between E and E_d based on Concrete Density (Popovics, 2008).*

Where:

- E = Static Modulus of Elasticity (psi)
- E_d = Dynamic Modulus of Elasticity (psi)
- K = 0.23 (psi)
- ρ = Density (lb/ft^3)

In addition to determining a relationship between E and E_d, Popovics also studied the relationship between E_d produced from UPV, and E_d produced from the resonant frequency

method. **Figure 2-1** below shows comparison of these values carried out on concrete and paste cylinders, with larger values of Poisson's Ratio assumed for the paste specimens.

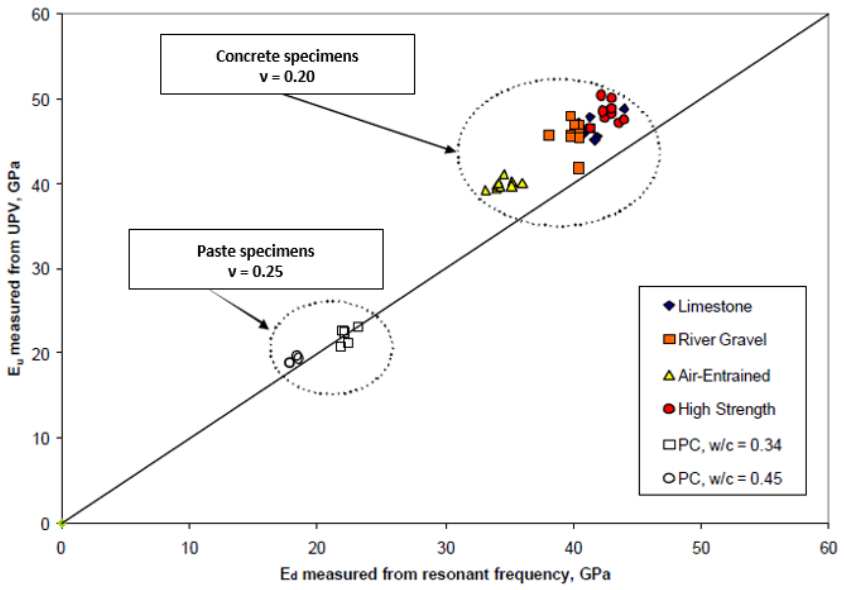

***Figure 2-1** – Comparison of E_d obtained from UPV, and E_d obtained from Resonant Frequency Analysis (Popovics, 2008).*

As seen in the above figure, E_d measured from UPV yielded a higher value than that measured from the resonant frequency method. Popovics also stated that of all the various resonant frequency methods, the longitudinal resonant frequency method on cylindrical concrete specimens produced the least accurate results (Popovics, 2008).

One possible reason for the difference between the Dynamic and Static Modulus is the composite nature of concrete. Popovics states that the static and dynamic moduli follow different mixture behaviors in composite elements, which would explain why the Dynamic Modulus is always greater than the Static Modulus. Popovics also observed that the difference between these moduli values was not detected in the paste specimen samples, as they are a much more homogenous material (Popovics, 2008).

Another study conducted by Chavhan and Vyawahare in 2015 from the B.N. College of Engineering in Maharashtra, India showed the relationship between E and E_d for various Self-Compacting Concrete mixes using both the UPV method and resonant frequency method. Comparing the results from the Static Modulus tests, they produced the following correlation:

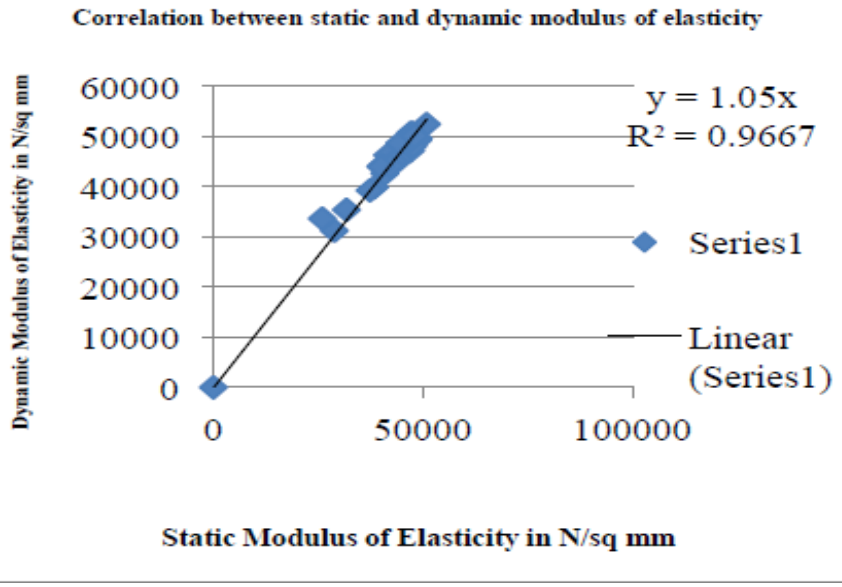

Figure 2-2 *– Correlation of Static and Dynamic Modulus in SCC (Chavhan & Vyawahare, 2015).*

Chavhan and Vyawahare determined that the Static Modulus E was approximately 5% less than that of the Dynamic Modulus, E_d (Chavhan & Vyawahare, 2015). They also showed that there tends to be a linear relationship between E and E_d for high strength SCC, as seen in **Figure 2-2**.

Another study, published by Salman & Al-Amawee in 2010, also indicated a linear relationship between E and E_d in both normal strength and high strength concrete mixes. The transverse impact resonance method was used to compute the Dynamic Modulus. In addition

to determining the correlation between E and E_d, the relationship between E_d and the compressive strength, f'_c was also determined. This relationship for normal strength concrete can be seen below in **Figure 2-3** (Salman & Al-Amawee, 2010). The legend indicates the various mixes that were used for the study.

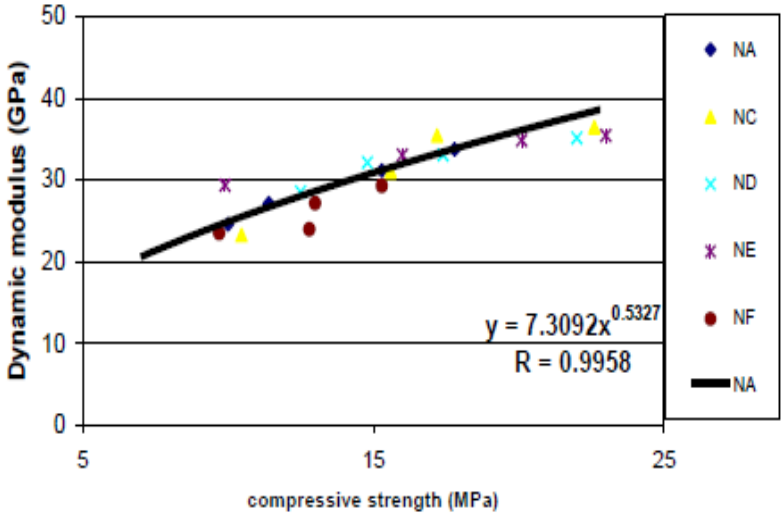

***Figure 2-3** – Relationship between E_d and $f'_{c'}$ (Salman & Al-Amawee, 2010)*

Based on this correlation, the authors were able to produce an empirical equation relating the two:

$$E = 7.3 f_c^{\,0.533}$$

***Equation 2-3** – Relationship between E_d and f'_c(Salman & Al-Amawee, 2010)*

As reported by previous research studies, the relationship between the Static Modulus of Elasticity and the Dynamic Modulus of Elasticity tends to be linear; however, the slope of the linear relationship differs. Larger aggregates in concrete results in higher strength concrete, and can affect the liner relationship between E and E_d. The type of concrete mix also affects this

correlation. As seen previously, self-compacting concrete produced different empirical relationships between E and E_d as compared to other traditional concrete mixes.

Understanding this linear relationship is important to the validity of the Dynamic Modulus tests, such as UPV and resonant frequency wave methods. Utilizing these methods as opposed to the Static Modulus test can save valuable time and money, and will continue to play a major role in NDT of concrete structures so long as the relationship between the two is understood.

2.2 – Ultrasonic Pulse Velocity Method

2.2.1 - Background of UPV Method

The ultrasonic pulse velocity (UPV) method used in concrete specimens is widely used to determine properties of concrete, such as the Dynamic Modulus of Elasticity. This method is based on the propagation of high frequency sound waves passing through the material. The wave speed is a function of the Dynamic Modulus of Elasticity, the density of material, the length of the specimen, and the Poisson's ratio of the concrete specimen (Lorenzi et. al, 2007). The wave frequencies are generally greater than 20 kHz.

During the UPV testing, the concrete specimens are in contact with a piezoelectric transducer on each side. Three different types of elastic wave propagation are produced from the transducer:

- Longitudinal waves (or P-waves)
- Surface waves (or Rayleigh waves)
- Shear waves (or transverse waves)

Longitudinal, or P-wave velocity is a factor of the material properties, such as Young's Modulus, Poisson's Ratio, and density. The particle motion of P-waves is parallel to the wave propagation of the specimen. P-waves are the fastest of the three waves (Dashti, 2016). Stronger and more durable materials have a higher magnitude P-wave velocity, thus resulting in stronger material properties. Air, water and some common materials used in the construction industry and their corresponding longitudinal wave velocities can be seen in **Table 2-1**:

Material	Longitudinal (P-Wave) Velocity (m/sec)
Air	331.5
Water	1490
Wood (Parallel to Grains)	4000 – 5000
Wood (Perpendicular to Grains)	1200 – 2400
Concrete	3000 – 5000
Steel	5000 – 6000

Table 2-1 *- P-Wave Velocities in Common Construction Materials (Halabe, et al. 1995)*

Surface waves, or Rayleigh waves, travel on the surface of the materials. The particle vibrations of these waves are more complex, and resemble elliptical particle displacement. These waves are determined to be the slowest of elastic waves. Transverse waves, or shear waves, have particle motion perpendicular to the wave propagation, and have been determined to be faster than the surface waves. (Dashti, 2016).

The longitudinal wave velocities for isotropic, homogeneous materials can be calculated using the following equation:

$$V = \sqrt{\frac{E(1-\nu)}{\rho(1+\nu)(1-2\nu)}}$$

Equation 2-4 *– Longitudinal Wave Velocity*

Where:

- *V = Longitudinal Wave Velocity (m/sec)*
- *E = Dynamic Young's Modulus of Elasticity (kN/m^2)*
- *v = Poisson's Ratio*
- *ρ = Mass Density (kg/m^3)*

The longitudinal wave velocity, *V*, can also be calculated from the following equation:

$$V = \frac{L}{T}$$

***Equation 2-5** – Additional Longitudinal Wave Velocity Equation*

Where:

- *V = Longitudinal Wave Velocity (m/sec)*
- *L = Specimen Length (m)*
- *T = Time Taken for Pulse to Travel Specimen Length (sec)*

The travel time, *T*, is obtained from the display unit of UPV setup, and is usually recorded in microseconds.

2.2.2 - UPV Testing Methods

Testing equipment for UPV must provide means of generating a pulse from the transducer that is transmitted into the concrete specimen. On the opposite side of the specimen, a receiver must receive and amplify the pulse and transmit to a display unit in which the travel time can be shown (Chapman & Hall, 1996). **Figure 2-4** shows the basic setup for a typical UPV setup. Repetitive voltage pulses are generated and then the transducer transforms the pulses into wave bursts of mechanical energy. The receiving transducer receives the

mechanical energy wave bursts and converts them back into voltage pulses of the same original frequency. An electronic timing device is able to measure the time interval between the transmitting transducer energy output and the receiving transducer energy input. The time interval is then displayed on an oscilloscope or display unit (Chapman & Hall, 1996).

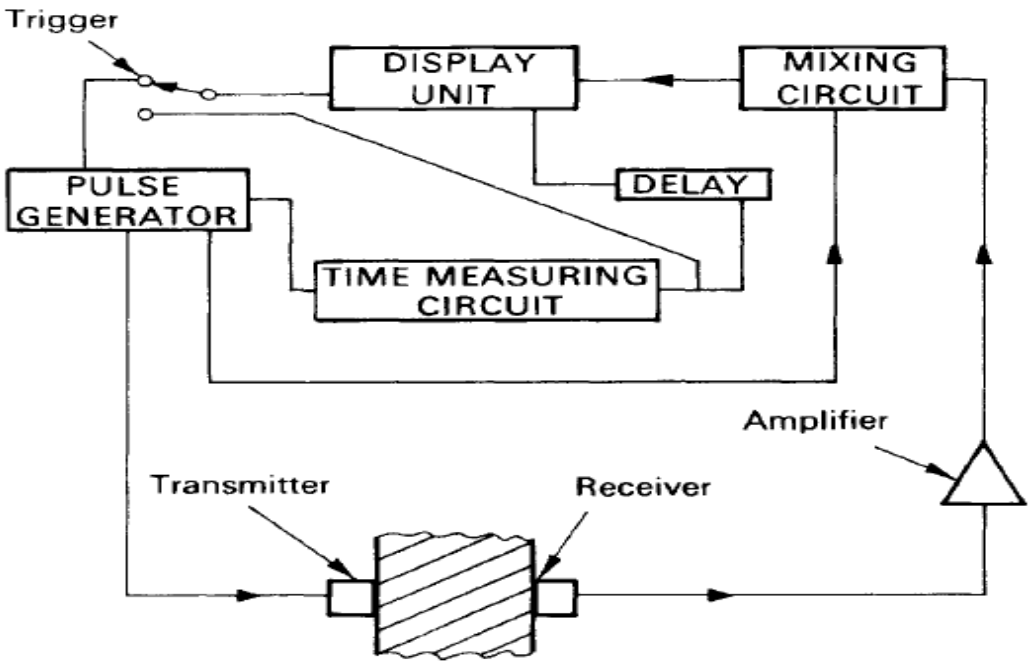

Figure 2-4 *– Standard UPV Equipment Setup (Chapman & Hall, 1996)*

It is also important that a good acoustical coupling is used between the transducer surface and the specimen surface to provide more reliable results. This is typically achieved by using some sort of medium, such as a petroleum jelly. Rougher surfaces may require a heavier medium, such as a thick grease. This helps to smooth out the surface of the specimen to ensure that the transducers are completely flush with specimen and the wave propagates completely through the specimen (Chapman & Hall, 1996).

2.2.3 - Factors Influencing UPV

Although Ultrasonic Pulse Velocity Testing is a viable means of determining the Dynamic Modulus of Elasticity, there are several factors that may influence the results. These may consist of human error, moisture content, steel reinforcement, admixtures, size, etc. Large defects and inconsistences on the finishing of the concrete samples can affect results as well. It is important to take into consideration these factors when engaging in a UPV test, and appropriate measures should be taken to minimize the effect of these factors on the overall results.

2.2.3.1 - Moisture Content

It was reported that moisture content has two types of effects on UPV; chemical and physical. When two different specimen types are cast, it is vital to ensure that the same curing conditions are used for both specimens. Significant differences in the pulse velocity can be seen in this case due to the hydration of the cement during the curing process. Presence of free water in the voids can influence the velocity as well (Guidebook on NDT of Concrete Structures, 2002). The moisture content should be monitored for the specimens throughout the entire testing period, and an effort to keep the moisture contents uniform for all the specimens should be made.

2.2.3.2 - Path Length

The path length that the pulse wave will travel, or the length of the specimen, can influence the resultant velocities for longer specimens. *The Guidebook on Non-Destructive Testing of Concrete Structures* (2002) suggests that the length should be long enough "not to be significantly influenced by the heterogeneous nature of the concrete." For aggregate size 20mm

or less, the minimum length should be 100mm. For aggregate size 20mm – 40mm, the minimum length should be increased to 150mm. The pulse velocity tends to reduce slightly as the length decreases. This is due to the increased attenuation of higher frequency components as opposed to lower frequency components. The shape of the onset of the pulse also tends to become more rounded with longer specimen lengths (Guidebook on NDT of Concrete Structures, 2002).

2.2.3.3 - Aggregate Type

It has been found that the size of aggregate in the specimens can influence the resultant pulse velocities. It has been seen that a higher aggregate content often produces a higher pulse velocity (Trtnik et al., 2008). This should be noted during the mix design.

2.2.3.4 - Defects

Various defects and heterogeneities in the concrete specimens can greatly affect the resultant pulse velocity. During the casting process, it is important to follow all the ASTM standards to avoid any defects or discontinuities from developing in the specimens.

The overall quality of the concrete can be determined from the longitudinal pulse velocity (in both S.I. and U.S Customary units) in **Table 2-2**

Longitudinal pulse velocity		Quality of concrete
km/s.10^3	ft/s	
>4.5	>15	excellent
3.5-4.5	12-15	good
3.0-3.5	10-12	doubtful
2.0-3.0	7-10	poor
<2.0	<7	very poor

Table 2-2 *- Concrete Classification Based on Longitudinal Pulse Velocity (Guidebook on NDT of Concrete Structures, 2002)*

The Ultrasonic Pulse Velocity Method has proven to be a viable means for determining key material properties of concrete specimens. It is a safe, non-destructive method that is widely used in a number of different applications. UPV will continue to be an important factor in structural engineering, especially in concrete-based structures.

2.3 – Impact Resonance Frequency Method

2.3.1 - Background of Impact Resonance Frequency Method

In this study, resonance frequency analysis was also conducted to calculate the Dynamic Modulus. Measuring resonance frequencies to determine material properties is a relatively new method of non-destructive testing. The resonant frequencies of vibration are related to the density and the Dynamic Modulus of Elasticity of the material. The resonance frequencies of the concrete specimens are determined by exciting the specimen in either the longitudinal, transverse, or torsional mode and then measuring the resultant free vibrations (Gudmarsson, 2014). Resonant frequencies are frequencies in which waves reflect off of the ends of the

specimens and add constructively (Lee, Kim & Kim, 1997). The impulse force and acceleration are recorded in the time domain, and then transformed to the frequency domain through Fast Fourier Transform (FFT). Frequency Response Functions (FRF) are then developed by the data acquisition and displayed on the screen. The resonant frequency can then be obtained from these FRFs (Placky, Padevet & Polak, 2009).

Flexural resonant frequencies are controlled by the boundary conditions of the specimen, and the dimensions of the specimens. It is vital that these parameters remain constant throughout the entire experimental procedure to reduce error and bias. ASTM says that there are two different methods to determine the resonant frequencies; the forced resonance method, and the impact resonance method. The impact resonance method is used for this study.

2.3.2 - Impact Resonance Frequency Testing Methods and Equation Derivation

In the impact, or impulse resonance frequency method, measuring the fundamental resonance frequency through either the transverse, longitudinal, or torsional vibrations depends on the dimensions of the specimens and impact point on the specimen (Placky, Padevet & Polak, 2009). The boundary conditions may differ for the specimens based on the direction. The different boundary conditions for each of these directions can be seen in **Figure 2-5**

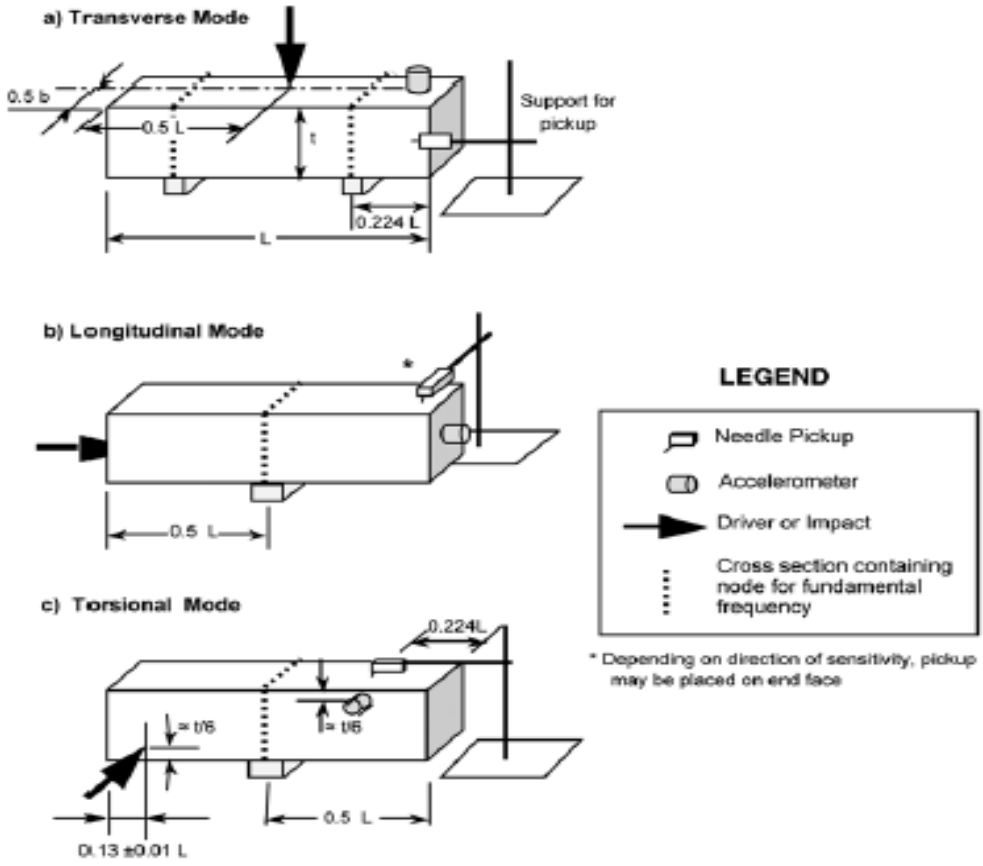

Figure 2-5 *- Boundary Conditions for Impact Resonance in a.) Transverse Mode, b.) Longitudinal Mode, and c.) Torsional Mode (ASTM 215-08)*

The basic set-up and configuration for the impact resonance test consists of an impact hammer and accelerometer, which are both connected to a signal conditioner. The signal conditioner is connected to the data acquisition device and converts the signals from analog to digital. The signal conditioner can also amplify the measurement signals if needed (Gudmarsson, 2014). The basic setup and configuration for the impact resonance test can be seen in **Figure 2-6**.

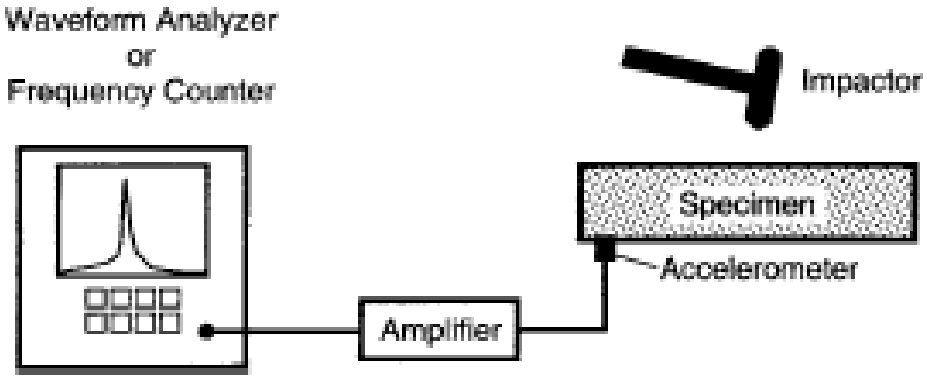

Figure 2-6 *- Impact Resonance Equipment and Configuration (ASTM 215-08)*

The boundary conditions and mode directions of the specimen dictate the location and direction of where the impact hammer will strike the specimen.

2.3.2.1 – Equation Derivation

In this study, the transverse resonant frequencies were used to calculate the Dynamic Modulus. The equation used to compute E_d from the transverse fundamental resonant frequencies is given from ASTM C215-08

$$E_d = CMf^2$$

Equation 2-6 *– Dynamic Modulus from Transverse Flexural Resonant Frequency, (ASTM C215-08)*

Where M is the mass of the prism, f is the fundamental flexural resonant frequency, and C is given by:

$$C = .9464\frac{L^3}{bt^3}T$$

Equation 2-7 *– Equation for C (ASTM C215-08)*

Where:

- L = Prism Length
- b,t = Cross-Sectional Dimensions of Prism
- T = Dimensionless Correction Factor

The derivation of this equation comes from Bernoulli-Euler equation of natural frequencies of a prismatic beam:

$$\omega = (\beta_1 L)^2 \sqrt{\frac{EI}{\rho A L^4}}$$

Equation 2-8 *– Natural Frequencies of a Prismatic Beam*

Where:

- $\beta_1 L$ = Function of Boundary Conditions
- E = Elastic Modulus
- I = Moment of Inertia of Cross Section
- ρ = Mass Density of Prism
- A = Area of Cross-Section
- L = Prism Length

Substituting in $f = \frac{\omega}{2\pi}$ and rearranging to solve for E yields the following equation:

$$E = Mf^2 \frac{L^3}{bt^3} \frac{48\pi^2}{(\beta_1 L)^4}$$

Equation 2-9 *– Elastic Modulus from Natural Frequencies Equation*

For a pinned-pinned beam, $\beta_1 L$ values are determined through the solution to the mode shape for a pinned-pinned beam. Values of $\beta_1 L$ for the first, second, and third mode are listed below respectively:

- $\beta_1 L = 4.7300$
- $\beta_2 L = 7.8532$
- $\beta_3 L = 10.9956$

Substituting the $\beta_1 L$ value into **Equation 2-9** for the first mode yields the final equation, identical to the ASTM equation apart from the correction factor, T

$$E = Mf^2 \frac{L^3}{bt^3}(.9464)$$

Equation 2-10 *- Elastic Modulus from Natural Frequencies with $\beta_1 L$ (First Mode)*

In a study titled "Equations for Computing Elastic Constants from Flexural and Torsional Resonant Frequencies of Vibration of Prisms and Cylinders" by Gerald Pickett in 1945, Pickett derived the elastic correction factor, T, to adjust the calculated modulus value for the material properties (Poisson's Ratio) and the finite thickness of the prism (Pickett, 1945). For L/t > 20, the modulus value calculated in **Equation 2-10** and the theoretical elastic modulus are in good agreement with each other as the equation is derived for a continuous beam. For L/t < 20, the beam is very short, and therefore the effect of shear forces and rotary inertia must be taken into account. Pickett generated the following equation to adjust the modulus value by for specimens with L/t <20 in the fundamental mode (Stubna, Trnik, 2006).

$$T = 1 + 6.585(1 + 0.0752\nu + 0.8109\nu^2)\left(\frac{t}{L}\right)^2 - 0.868\left(\frac{t}{L}\right)^4 - \left[\frac{8.340(1+0.2023\nu+2.173\nu^2)(\frac{t}{L})^4}{1.000+6.338(1+0.1408\nu+1.536\nu^2)(\frac{t}{L})^2}\right]$$

Equation 2-11 *– Correction Factor T for Elastic Modulus (Pickett, 1945)*

Where v is the Poisson's Ratio of the concrete. Calculated T values are given in a table in ASTM C215-08 for specific Poisson's Ratio and K/L values.

2.3.3 - Factors Affecting Impact Resonance Frequency Test

The Impact Resonance Frequency Method has proven to be a reliable technique to determine various properties in concrete specimens. However, there are a number of factors that could influence or skew the results from the tests. It is vital that the ASTM Standard for Resonant Frequencies of concrete specimens is followed in order to obtain accurate results from the experiment.

In one study from the KSCE Journal of Engineering, it was found that concrete curing conditions had a slight effect on the produced resonant frequencies. It was seen that at any given time, the fundamental resonant frequency was slightly higher for specimens that were cured in wet conditions versus those that were cured in air dry conditions. This resulted in a larger Dynamic Modulus for the specimens (Lee, Kim & Kim, 1997).

Mixture proportions can influence the fundamental resonance frequency and the resulting Dynamic Modulus. Aggregate properties can also influence the results. Specimen size is another important factor to be considered (Klieger and Lamond, 1994).

2.3.4 – Limitations of Resonant Frequencies

Although the Impact Resonant Frequency Method is useful and quite simple to perform on concrete specimens, there are several major limitations to this technique. The impact test is generally tested on small concrete prisms or cylinders (around 3in x 4in by 16 in). The frequency results produced on these specimens could be greatly different than those produced from in situ structures in the field because of the boundary conditions. While attempts are made to reduce the effect of these boundary conditions, they will always influence the fundamental resonant frequencies that are obtained (Klieger and Lamond, 1994).

The other main limitation of this technique has to do with the equations used to calculate the Dynamic Modulus. The equations include correction factors based on the shape of the specimen. These shape factors are limited to either cylinders or prims and are not available for any other complex shape, or require intricate correction factor determination (Klieger and Lamond, 1994).

Aside from the limitations mentioned above, the Impact Resonance Frequency Method provides a valid means of determining the Dynamic Young's Modulus, among other concrete properties. The method can also be used to study deterioration of concrete that is subjected to freeze-thaw conditions. Studies have also been done using this method to determine fire-related damage and deterioration of concrete (Klieger and Lamond, 1994).

2.4 – Self-Consolidating Concrete

2.4.1 – Background/History of SCC

One of the concrete mixes used in this study is a Self-Consolidating Concrete mix. Self-Consolidating Concrete was first developed in 1988 (Okamura and Ouchi, 2003). It is a newer, innovative concrete mix that is being used all throughout the world in a wide variety of different structural applications. SCC is an extremely flowable and non-segregating mix that can easily spread into place without any additional mechanical consolidation (Daczko, 2012). The idea for SCC first arose in 1986 by Professor Hajime Okamura of Kochi University of Technology in Japan. The idea was an attempt at a solution for growing durability concerns of concrete from the Japanese government. Initial research determined that the root of the durability problems in structures was inadequate concrete consolidation during the casting phase (Vachon, 2002). Normal consolidation of concrete requires the use of some sort of internal vibrators to help spread out the concrete mix once it has been poured into the formwork. The idea behind SCC is that the mix would consolidate on its own and would require no vibration assistance. Eliminating this consolidation problem from concrete, Okamura found that the durability in structures would be greater than that of traditional vibrated concrete.

When structures and formwork contain a large quantity of steel reinforcement, or rebar, it is extremely difficult to ensure that concrete has completely consolidated and formed around the reinforcement without creating any voids. Manual and mechanical vibrating methods have proved inefficient, expensive, and time consuming (Self Compacting Concrete, 2010). As the size of structures continue to increase, and areas of construction become more congested, SCC has proven to be a very viable and inexpensive means of efficiently compacting concrete

without having to use any additional vibrating technology. Due to the extremely low viscosity of SCC, voids and honeycombs can be minimized/eliminated in structures. This ultimately can lead to greater freedom in design for structural engineers, along with safer working conditions (EFNARC, 2002).

2.4.2 – Mix Design Requirements

There are three main characteristics that SCC must possess to meet the stated workability requirements (Gurjar, 2004).

- *Filling Ability: Ability to flow and completely fill all voids and spaces within the formwork under its own weight.*
- *Passing Ability: Ability to flow through tight spaces (such as between reinforcements) without segregation occurring.*
- *Segregation Resistance: Ability to remain homogenous during the transportation and casting.*

In one study published in *Construction and Building Materials* by Dr. Roger Chen and Joseph Sweet in 2012, SCC was used to cast caissons on the Stalnaker Run bridge, a rural bridge replacement project in Elkins, WV. (Chen & Sweet, 2012). In addition to casting SCC elements, traditional concrete was also used to cast identical elements for comparison. The mix designs for both traditional and SCC can be seen below in **Table 2-3**.

Component	Traditional caisson mix	SCC-1 caisson mix
Type I cement[a]	564 (334)	638 (378)
Class F Fly Ash[a]	70 (42)	112 (66)
Water[a]	250 (148)	285 (169)
Coarse aggregate[a]	1743 (1034)	1400 (830)
Fine aggregate[a]	1220 (723)	1388 (823)
w/cm	0.394	0.381
AEA[b]	2.0 (130.4)	0.35 (22.8)
Type A (D) WRA[b]	6.0 (391.2)	–
Type F HRWRA[b]	–	4.5 (293)
Type S VMA[b]	–	0.75 (49)
Type D retarder[b]	–	5.0 (326)

[a] lb/yd^3 (kg/m^3).
[b] oz/100 lb Cementitious materials (mL/100 kg).

Table 2-3 *– Mix Designs used for the Stalnaker Run Bridge Caissons (Chen & Sweet, 2012).*

In addition to the components for the traditional mix, high range water reducer, viscosity modifying agents, and retarder were all used in the SCC mix. It should also be noted that Fly Ash was used in this mix as a supplementary cementitious material.

2.4.3 –Mechanical Properties of SCC

It is important to determine the mechanical properties of Self-Consolidating Concrete at different ages, such as compressive strength, tensile strength, Young's Modulus, etc. to obtain a better understanding of how effective the mix can be.

2.4.3.1 – Compressive and Tensile Strength

It has been seen through previous studies that the 28-day strength of SCC and traditional vibrated concrete is similar, however, in some cases it has been seen that at the same water to cement ratios, SCC produces a much higher compressive strength (Theran, 2008). In regards to tensile strength, SCC tends to provide higher strength than that of traditional concrete mixes. The basis of this is that SCC has a better microstructure, a smaller total porosity, and more pore size distribution within the interfacial transition zone of SCC. The

use of different cementitious materials, such as flyash, in SCC could result in different strength properties, both compressive and tensile (Theran, 2008).

2.4.5.2 – Modulus of Elasticity

There have been many research studies to compare the Modulus of Elasticity in SCC and traditional vibrated concrete. In many studies, it has been seen the modulus for SCC can be up to 10% to 15% lower than that of conventional concrete. On the contrast, some studies have shown that conventional concrete with the same compressive strength of SCC results approximately the same modulus of elasticity (Theran, 2008).

Overall, there has been no consensus in the relationship of Modulus of Elasticity between SCC and conventional concrete mixes. As SCC continues to become more widespread and the mix designs continue to advance, an understanding on this relationship should arise.

Chapter 3 Laboratory Experimental Procedures & Results

3.1 – Mix Design and Concrete Casting

There were four total concrete castings that were conducted at the Concrete Research Laboratory at West Virginia University for this study. The first casting was a 50% slag batch, in which 50% of the weight of cementitious material was slag, and 50% was ordinary Portland cement. The second casting was a 30% flyash batch, in which 30% of the weight of cementitious material was flyash, and 70% was Portland cement. The third casting was conventional ordinary Portland cement concrete (OPC). The fourth and final casting was a self-consolidating concrete (SCC) mixture. All concrete castings were conducted in-house, along with all experimental procedures and analysis. The ASTM Standard for Making and Curing Concrete Test Specimens in the Laboratory was followed to develop each of the different concrete batches, and form the appropriate specimens for each. (ASTM C192/C 192M, 2006). A standard laboratory drum mixer with a capacity of $3.0ft^3$ was used in accordance with ASTM for all samples.

The materials used in each of the castings were ordered from Central Supply Company, a local concrete production company in the Morgantown, WV. These materials consisted of cement, flyash, slag, sand and large aggregate. The drum mixer and setup for the 50% Slag casting can be seen below in **Figure 3-1**.

Figure 3-1 *– Drum Mixer, Materials, and Slump Test Setup – 50% Slag Casting*

After the concrete was produced in the drum mixer, air content, slump, and water/cement ratio for each concrete batch were determined. The concrete was placed into the respective molds/forms with appropriate rodding and consolidating techniques outline by ASTM (ASTM C192/C 192M, 2006). After the molds were filled, damp burlap was placed over top of each of the specimens for a 24-hour period.

24 hours after each of the castings, the concrete specimens were removed from their respective molds, and placed into curing tanks filled with water and a lime additive. The temperature of the curing tanks was monitored with temperature loggers to ensure that the temperature was a constant 72°F for each of the samples.

3.1.1 – 50% Slag Batch

The first concrete batch to be cast was the 50% Slag mixture, cast on September 23, 2016 at approximately 10:00 A.M. A total of 2.5ft^3 was produced during this casting. The specimens that were formed are as followed:

- 2 - 6” x 12” Cylinders
- 17 – 4” x 8” Cylinders
- 3 – 3” x 4” x 16” Rectangular Steel Mold Prims

The 6” x 12” Cylinders were used in the experiment to determine the Static Young’s Modulus. The 4” x 8” cylinders were used to measure the compressive strength. The rectangular prisms were used to determine Dynamic Young’s Modulus through the Ultrasonic Pulse Velocity method experiment, and the Impact Resonance Frequency method experiment.

Approximately 0.01 ft^3 of concrete was also used for the air content test. This concrete could not be reused as additional water was added to the concrete during the procedure, thus the concrete was compromised.

Prior to the production of the concrete batch, the sand and aggregate dried in an oven for approximately 36 hours, and was then transferred to a sealed cooling tank for an additional 24 hours. This ensured that the moisture content would have no effect on the water cement ratio or the strength of the concrete. A water to cement ratio of 0.42 was controlled for all concrete mixes, and therefore was not variable.

The mix design for the 50% slag casting per cubic yard can be seen in **Table 3-1** below:

50% Slag Batch Mix Design		
Material	**Unit Weight**	
Sand	**1364**	lb/yd^3
#57 Aggregate	**1795**	lb/yd^3
Slag	**254**	lb/yd^3
Cement	**254**	lb/yd^3
Water	**215**	lb/yd^3
AEA92 - Air	**0.4**	Per CWT
EuconWR	**3**	Per CWT
Retarder	**1.3**	Per CWT

Table 3-1 *- Mix Design for 50% Slag Concrete Mixture per yd^3*

3.1.2 – 30% Flyash Batch

The second concrete batch that was cast was the 30% Flyash batch, cast on October 12, 2016 at approximately 9:00 A.M. The materials for this batch were provided from District 10 in West Virginia, as part of an ongoing research study at West Virginia University. Three different batches were completed using the 30% flyash mixture. The specimens that were formed as a part of this research project are as followed:

- 2 - 6” x 12” Cylinders (One from Batch 1, & One from Batch 2)
- 20 – 4” x 8” Cylinders (Combination from each of the 3 Batches)
- 2 – 3” x 4” x 16” Rectangular Steel Mold Prims (1 from Batch 2, & 1 from Batch 3)

The 6” x 12” Cylinders were used in the experiment to determine the Static Young’s Modulus. The 4” x 8” cylinders were used for the compressive strength. The rectangular prisms were used to determine Dynamic Young’s Modulus through the Ultrasonic Pulse Velocity method experiment, and the Impact Resonance Frequency method experiment.

Similar to the 50% slag batch, the sand and # 67 aggregate was placed in the oven for 36 hours, and cooled for an additional 24 hours prior to casting. The mix design per cubic yard that was used for flyash concrete batch can be seen in **Table 3-2** below:

30% Flyash Mix Design		
Material	**Weight**	
Sand	**1360**	lb/yd^3
#67 Aggregate	**1780**	lb/yd^3
Flyash	**168**	lb/yd^3
Cement	**340**	lb/yd^3
Water	**215**	lb/yd^3
AEA92 - Air	**0.56**	Per CWT
EuconWR	**3**	Per CWT
Retarder	**3**	Per CWT

***Table 3-2** - Mix Design for 30% Flyash Concrete Mixture per yd^3*

3.1.3 – OPC

The third concrete batch that was cast was an Ordinary Portland Cement (OPC) Concrete batch, cast on October 24, 2016 at approximately 8:00 A.M. A total of 2.5ft^3 was produced during this casting. The specimens that were formed are as followed:

- 2 - 6” x 12” Cylinders
- 20 – 4” x 8” Cylinders
- 2 – 3” x 4” x 16” Rectangular Steel Mold Prims

The 6” x 12” Cylinders were used to in the experiment to determine the Static Young’s Modulus. The 4” x 8” cylinders were used to measure the compressive strength. The

rectangular prisms were used to determine Dynamic Young's Modulus through the Ultrasonic Pulse Velocity method experiment, and the Impact Resonance Frequency method experiment.

The sand and #57 aggregate was placed in the oven for 36 hours to completely dry, and then placed in cooling tanks for 24 hours to cool prior to casting. The mix design per cubic yard for the OPC batch can be seen below in **Table 3-3**:

OPC Batch Mix Design		
Material	**Weight**	
Sand	**1424**	lb/yd^3
#57 Aggregate	**1633**	lb/yd^3
Cement	**564**	lb/yd^3
Water	**235**	lb/yd^3
AEA92 - Air	**0.4**	Per CWT
EuconWR	**4.5**	Per CWT

***Table 3-3** - Mix Design for OPC Concrete Mixture per yd^3*

3.1.4 – SCC

The fourth and final concrete batch that was cast was Self-Consolidating Concrete (SCC), cast on January 12, 2017 at approximately 11:00 A.M. a total of 2.3 ft^3 was produced during the casting. The specimens that were formed are as followed:

- 2 – 6" x 12" Cylinders
- 8 – 4" x 8" Cylinders
- 1 – 3" x 4" x 16" Rectangular Steel Mold Prims

Prior to casting, the moisture content of the fine aggregate was determined, in order to calculate the quantities for the mix design. The mix design for the SCC batch per cubic yard can be seen below in **Table 3-4**:

SCC Batch Mix Design		
Material	**Weight**	
Sand	**1415**	lb/yd^3
#67 Aggregate	**1469**	lb/yd^3
Cement	**735**	lb/yd^3
Water	**284**	lb/yd^3
Silica Fume	**75**	lb/yd^3
Glenium 750 (HRWR)	**10**	Per CWT
VMA 362	**3**	Per CWT
MBVR (Air)	**1.5**	Per CWT

Table 3-4 *– Mix Design for Self-Consolidating Concrete per yd^3*

For the SCC mix, first the large aggregate was blended with a small amount of the required water in the drum mixer. Next, the fine aggregate, cement, silica fume, and remaining water was mixed into the drum mixer for approximately 3 minutes. The mixture was then allowed to rest for 2 minutes. Lastly, the admixtures were added to the drum mixer, and mixed for an additional 2 minutes until the mix provided typical characteristics of SCC.

3.2 – Tests During Castings

After all materials have were thoroughly mixed in the drum mixer, the slump and air content was measured for each concrete mix. The water to cement ratio was also measured to confirm that it was the same as the design.

3.2.1 – Slump Test

The standard Slump test for Hydraulic-Cement Concrete was performed on the 50% Slag batch, 30% Flyash batch, and the OPC batch. A different version of this test was done for the SCC batch due to its extreme flowability. The slump test is an experimental test that is commonly used in the field to determine the workability and overall consistency of the fresh concrete mix. It is typically performed immediately after the concrete has been mixed to provide the most accurate results.

For each of the concrete batches, the ASTM Standard for Slump Test was followed (ASTM C143, 2010). The freshly mixed concrete is compacted into the standard slump cone (seen in **Figure 3-2** and **Figure 3-3**). The cone is then removed slowly (5-7 seconds should elapse) and the difference in height is immediately measured to determine the slump value.

The Slump values for each of the three applicable concrete batches is seen in **Table 3-5**. The common range for slump measurement is anywhere from 2 in. to 7 in., with the lower end of the range resulting in less workability, and the higher range resulting in greater workability.

Slump Measurements	
Concrete Type	**Slump (in.)**
50% Slag	6.75
30% Flyash (Batch 1)	5.25
30% Flyash (Batch 2)	5.00
OPC	8.25

***Table 3-5** – Slump Measurements for Concrete Batches*

As seen in the table, the Slag and Flyash batches all have slump values within the acceptable range. The OPC had a slump of 8.25 inches, indicating that the batch may have been

too flowable, and could result in a reduction of strength for the batch. The basis for this high slump was an excess of air entraining agent added to the mix.

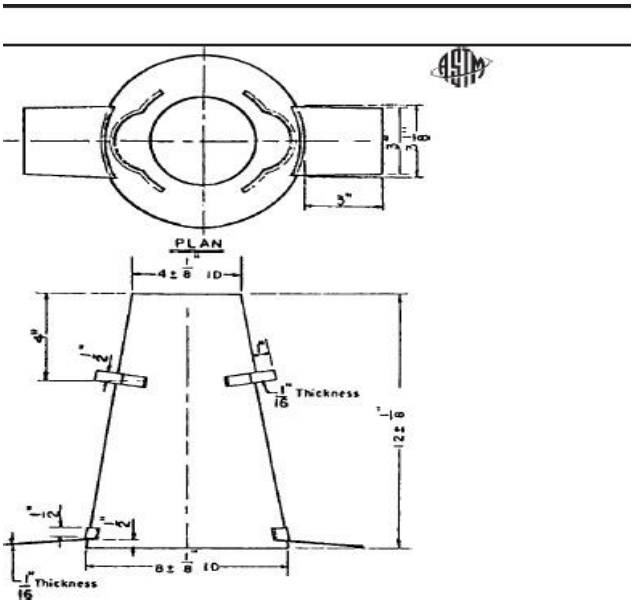

Figure 3-2 *– Standard Slump Cone Mold (ASTM C143, 2010).*

Figure 3-3 *– Slump Test Result for 50% Slag Batch*

3.2.2 – Air Content Test (Pressure Method)

The purpose of the air content test is to determine the percentage of air that is contained in the freshly mixed concrete, excluding any air that may exist inside voids of aggregate. The measured air content can be a factor of consolidation techniques, exposure, uniformity of air bubbles, amongst other variables (ASTM C231, 2003). Air content is important as it can be directly related to the strength and freeze-thaw durability of the concrete. Typically, concrete with a lower air content results in a higher strength concrete, and vice-versa.

There are two types of air content apparatus' commonly used to determine air content in freshly mixed concrete, Type A and Type B meters. For the purpose of this research project, a Type B Meter was used. A schematic of this apparatus can be seen in **Figure 3-4** below, and the actual apparatus used in each of the castings can be seen in **Figure 3-5**.

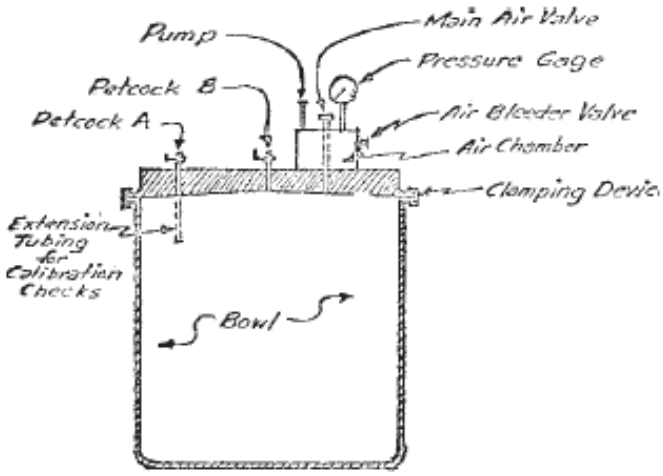

Figure 3-4 *– Type B Air Content Apparatus (ASTM C231, 2003).*

Figure 3-5 *– Determining the Air Content of 50% Slag Batch using Type B Air Content Apparatus*

The air content apparatus was calibrated appropriately according to the ASTM C231 Standards (ASTM C231, 2003). The freshly mixed concrete was then placed into the apparatus bowl, rodded, and finished accordingly. The air content for each of the different concrete batches can be seen in **Table 3-6** below:

Air Content	
Concrete Type	**Air Content (%)**
50% Slag	4.3%
30% Flyash (Batch 1)	7.6%
30% Flyash (Batch 2)	7.6%
OPC	11.0%
SCC	2.6%

Table 3-6 *- Air Content for Concrete Batches*

As seen in the table, the air content for the OPC batch was excessively high, which would indicate that the strength would be reduced. This was due to the excess or air entraining agent added to the mix. A similar assumption was made for the OPC batch based on the high slump. The SCC batch had an air content of only 2.6%, which is low, however most SCC mixes

result in lower air contents which result in the higher compressive strength that is typically seen. The Slag and Flyash batches both have air content values within the acceptable range.

3.2.3 – SCC Tests During Casting

Upon completion of the Self Consolidating Concrete batch, a total of four quality control tests were completed to determine the overall quality of the mix. The slump flow test, T_{20}, J-Ring Flow test, and L-Box Test were all completed prior to casting.

3.2.3.1 – Slump Flow

One of the most common quality control tests for Self-Consolidating Concrete is the Slump Flow test. The Slump Flow test is used to determine the flowability and stability of the freshly mixed concrete. The same apparatus used in the traditional slump test on traditional vibrated concrete is used for the slump flow test. The cone was placed onto a rigid, wooden plate, with concentric circles marked on the plate to indicate where the 20in. diameter is, and the location of the slump cone. The process is outlined in ASTM C1611, and was followed during this procedure (ASTM C1611, 2014). Once the cone was filled with SCC (note, no vibration or rodding techniques were needed), the cone was slowly removed, lifting approximately 3 inches per second, allowing the concrete mix to flow out onto the board. Once the flow had stopped, the largest diameter was measured, along with the diameter perpendicular to the first measurement. The slump flow was then calculated by taking the average of the 2 perpendicular diameters. The slump flow for this mix was determined to be **22.5 inches**, which fell within the acceptable range of 22-30 inches. The slump flow and measurements can be seen below in **Figure 3-6**:

***Figure 3-6** – Slump Flow Measurement (d_1)*

3.2.3.2 – T_{20}

During the slump flow test, the T_{20} test is used synchronically as a measure of the viscosity of the concrete mix. Once the slump cone is removed, the time measured for the concrete flow to reach the 20 in. diameter circle on the platform is recorded (T_{20}). The T_{20} for the mix was determined to be **5.8 seconds**, which fell within the acceptable range of 2 -7 seconds (Dashti, 2016). This verified that the mix had acceptable viscosity and good flowability.

3.2.3.3 – J-Ring

The J-Ring test for Self-Consolidating Concrete is outlined in ASTM C1621. It is used to measure the passing ability of the concrete mix. The apparatus used is a rigid steel ring, 12 inches in diameter, with sixteen evenly spaced 5/8" diameter steel rods protruding from the ring (ASTM C1621, 2013). The same slump cone used in the slump flow test is used, however, the cone is inverted and placed in the direct center of the J-Ring Apparatus on the wooden platform. Once the cone was filled with the SCC mix, the cone was lifted 9 inches over a 3

second duration, allowing the concrete to flow outwards and pass between the steel rods. Similar to the slump flow test, the largest diameter of the spread and the diameter perpendicular were measured, and the average was calculated to determine the J-Ring slump flow. For this test, the slump flow was measured at **17 inches.** The difference between the slump flow and the J-ring slump flow was thus determined to be **5.5 inches**. The J-ring apparatus and slump flow can be seen in **Figure 3-7** below:

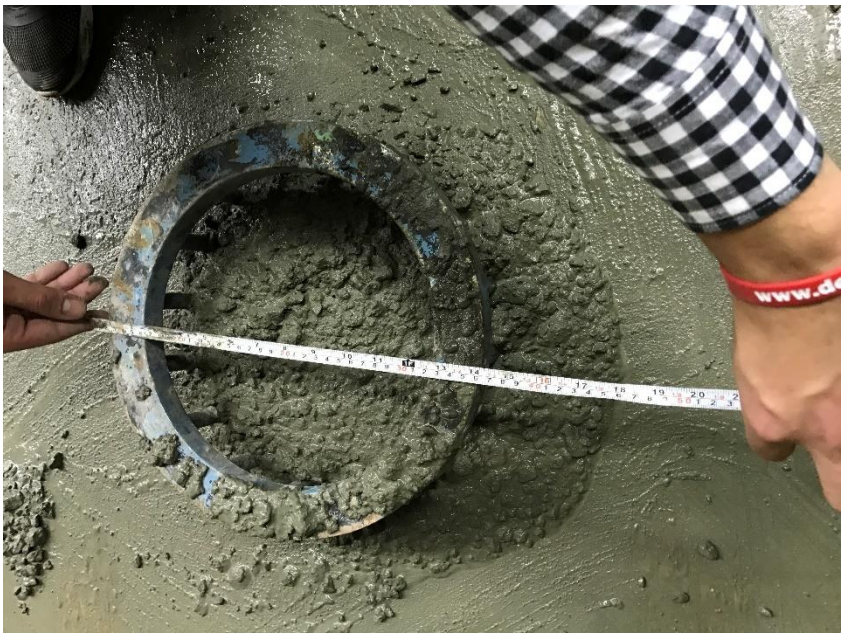

Figure 3-7 *– J-Ring Apparatus and Slump Flow*

The measured difference of 5.5 in. exceeded the acceptable range of 0 – 2 inches. This indicates that the SCC mixture did not have good passing ability, and had noticeable blocking properties (ASTM C1621, 2013). Adding a greater quantity of VMA's could help result in a reduction of blocking, and a better passing ability. The J-ring apparatus also had a large build-up of hardened concrete along some of the steel rods, which may have resulted in the higher value.

3.2.3.4 – L-Box

The final quality control test that was done on the self-consolidating concrete mix was the L-Box test. This test is used to determine the overall flowability and resistance to blocking for the mix. As described earlier in the literature review section, the apparatus that is comprised of an L-shaped steel vessel with a sliding gate on the bottom of the vertical section. Reinforcement bars are vertically mounted at the mouth of the horizontal section. The concrete was filled into the vertical section of the vessel, and allowed to set for 60 seconds prior to opening the gate. Once the gate was opened, the concrete could flow through the mouth of the horizontal section and through the reinforcement bars. The L-Box apparatus used in this experiment can be seen below in **Figure 3-8**:

***Figure 3-8** – L-Box Apparatus after Concrete Flow*

Once the concrete had stopped flowing, two measurements were recorded: the height of the mix at the end of the horizontal section, h_2, and the height of the mix in the vertical

section, h_1. The blocking ratio is then calculated by taking the ratio of h_2/h_1. For this experiment, it was determined that the blocking ratio was **0.62.** The acceptable range for blocking ratio is 0.80 – 0.85, therefore this mixture is susceptible to blocking. The addition of VMAs could help to increase the blocking ratio, and result in higher flowability of the SCC.

3.3 – Experimental Tests/Procedures

For this research study, the concrete specimens from each concrete batch were tested under several different ASTM experimental procedures at different ages. The concrete specimens were tested at 1, 3, 7, 14, and 28 days for the following:

- Compressive Strength
- Static Modulus of Elasticity
- Dynamic Modulus of Elasticity - Pulse Velocity Method
- Dynamic Modulus of Elasticity - Impact Resonance Frequency Method

Each of the concrete specimens remained in the same curing tank at a constant temperature of 72° F during the entire 28-day span when they were not undergoing testing.

3.3.1 – Compressive Strength Test

For each concrete batch, two 4” x 8” cylindrical specimens were tested at each of the above-mentioned days for compressive strength at the Concrete Materials Laboratory at West Virginia University. The ASTM Standard for Compressive Strength of Cylindrical Concrete Specimens (ASTM C39) was followed for each testing (ASTM C39, 2003). Each specimen was loaded under a uni-axial load under a constant loading rate until failure

The compressive strength for 50% Slag, 30% Flyash, OPC, and SCC can be seen below in **Table 3-7** below:

Measured Compressive Strength (psi)				
Test Day	**50% Slag**	**30% Flyash**	**OPC**	**SCC**
1	1,345	1,890	1,850	4,417
3	3,310	3,657	3,462	6,704
7	4,854	4,297	4,218	8,316
14	6,107	4,695	4,974	9,311
28	6,605	4,755	5,491	10,584

Table 3-7 *– Compressive Strength of Slag, Flyash, OPC and SCC Concrete MIxes*

As seen from **Table 3-7**, the compressive strength for SCC is the greatest compared to that of the other three mixes. In fact, it was almost double the strength of the other three concrete batches. At early ages, the flyash mix had a higher compressive strength compared to OPC and Slag, however the 28-day strength was the lowest of all four batches. It is typical of a flyash mix to have high early age strength. **Figure 3-9** shows the relationship of the compressive strength and concrete age for all four of the concrete mixes.

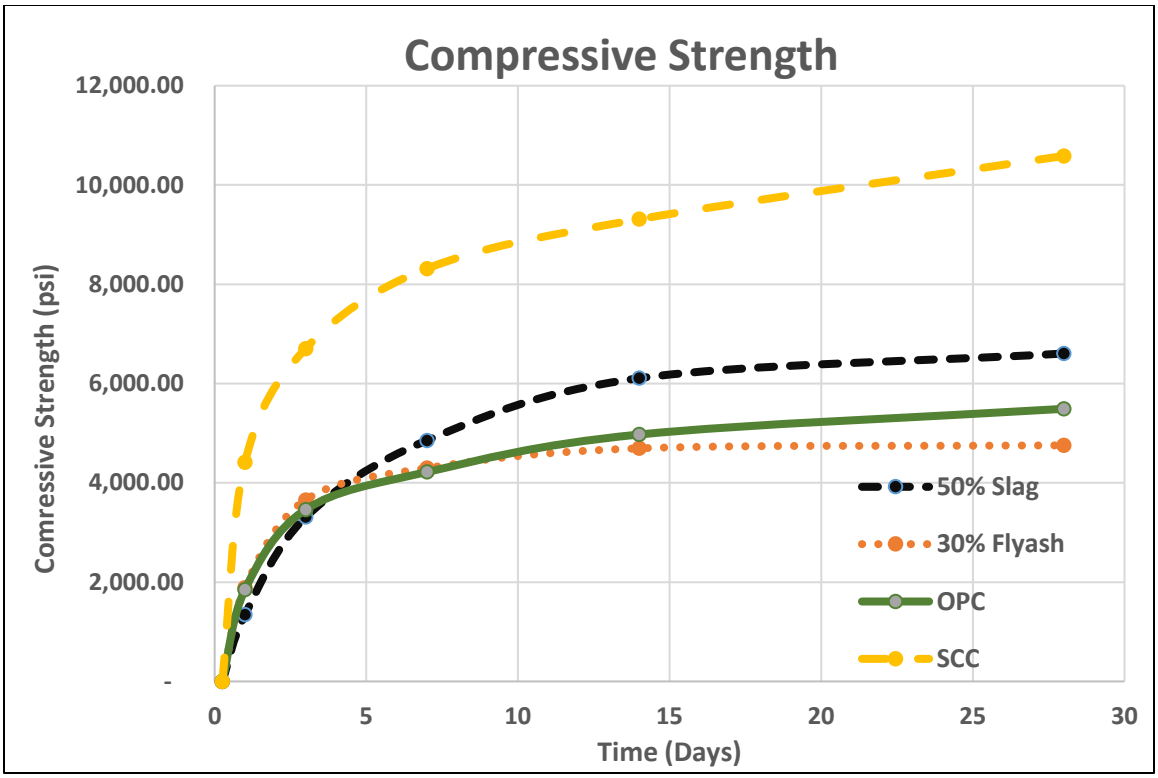

Figure 3-9 *– Relationship of Compressive Strength and Age of Slag, Flyash, OPC and SCC Concrete Mixes*

3.3.2 – Static Modulus of Elasticity

For each of the concrete batches, two 6" x 12" cylindrical concrete specimens were tested at 1, 3, 7, 14, and 28 days using the "Standard Test Method for Static Modulus of Elasticity and Poisson's Ratio of Concrete in Compression" (ASTM C469, 2002). Following the ASTM standard, the apparatus attached to each specimen consisted of a compressometer and an extensometer. The compressometer is used to measure the axial deformation of the specimen for the associated applied load. Based off these variables, the Static Modulus can then be calculated. The extensometer measures the transverse strain on the specimen from the applied loading. The transverse strains can then be used to calculate Poisson's Ratio of the

concrete. **Figure 3-10** shows the apparatus that was used for this procedure, consisting of the compressometer and extensometer.

Figure 3-10 *– Static Modulus Apparatus Consisting of Compressometer Gage (Dial Gage) and Extensometer Gage (Digital Gage)*

Once the apparatus is attached to the specimen, the specimen is loaded at a constant compressive rate, until 35% of the compressive strength has been reached. This maximum applied loading was determined from taking 35% of the compressive strength determined from the Standard Compressive Strength Test completed prior to the Static Modulus Test. The applied load was recorded once the strain gage reading was .0005. The strain gauge reading was also recorded once the compressive load had reached 35% of the compressive strength. To calculate the Static Modulus, the axial deformation must first be calculated based on the strain gage values. Axial deformation can be calculated using the following formula:

$$d = \frac{g e_r}{e_r + e_g}$$

Equation 3-1 *– Axial Deformation for Static Modulus of Elasticity Test (ASTM C469, 2002).*

Where:

- **d** = Total deformation of the specimen throughout the gage length (µin.)
- **g** = gage reading (µin.)
- **e_r** = perpendicular distance, measured in inches to the nearest 0.01 from the pivot rod to the vertical plane passing through the two support points of the rotating yoke
- **e_g =** the perpendicular distance, measured in inches, to the nearest 0.01 in. from the gage to the vertical plane passing through the two support points of the rotating yoke

The values for e_r, e_g, and d can be visualized from **Figure 3-11** below:

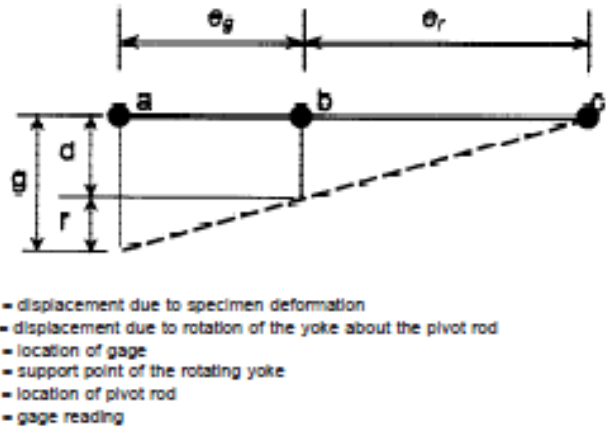

Figure 3-11 *– Diagram of Displacements from Static Modulus Apparatus (ASTM C469, 2002).*

Once the deformations were calculated, the Static Modulus of Elasticity can then be calculated based on to the slope of the stress strain curve. The formula for Static Modulus of Elasticity is seen in **Equation 3-2** below:

$$E = \frac{S_2 - S_1}{\epsilon_2 - 0.000050}$$

Equation 3-2 *– Static Modulus of Elasticity Formula (ASTM C469, 2002).*

Where

- E = Static (Chord) Modulus of Elasticity (psi)
- S_2 = Stress corresponding to 35% of Ultimate Compressive Load (psi)
- S_2 = Stress corresponding to a longitudinal strain, ϵ_1 of 50 millionths (psi)
- ϵ_2 = Longitudinal strain produced by stress, S_2

The results from the Static Modulus of Elasticity test for each of the four concrete mixes can be seen below in **Table 3-8**:

Static Modulus Comparison (psi)				
Test Day	**50% Slag**	**30% Flyash**	**OPC**	**SCC**
1	3.82E+06	4.17E+06	4.08E+06	4.88E+06
3	5.07E+06	4.96E+06	4.85E+06	5.48E+06
7	5.65E+06	5.16E+06	5.09E+06	5.88E+06
14	5.98E+06	5.48E+06	5.49E+06	6.23E+06
28	6.34E+06	5.64E+06	5.71E+06	6.54E+06

Table 3-8 *– Static Modulus of Elasticity for Slag, Flyash, OPC, and SCC Concrete Mixes*

Figure 3-12 shows the relationship of concrete age and Static Modulus for each of the different concrete mixes. Similar to the compressive strength, the Static Modulus was highest for the SCC batch as compared to the other three mixes. However, the modulus was not significantly greater than the 50% slag batch. The Flyash batch resulted in the lowest Static Modulus, however, extremely close to that of the OPC batch. It can also be seen that Flyash

concrete mix had a higher day 1 Modulus compared to OPC and slag, however, the strength plateaued with age.

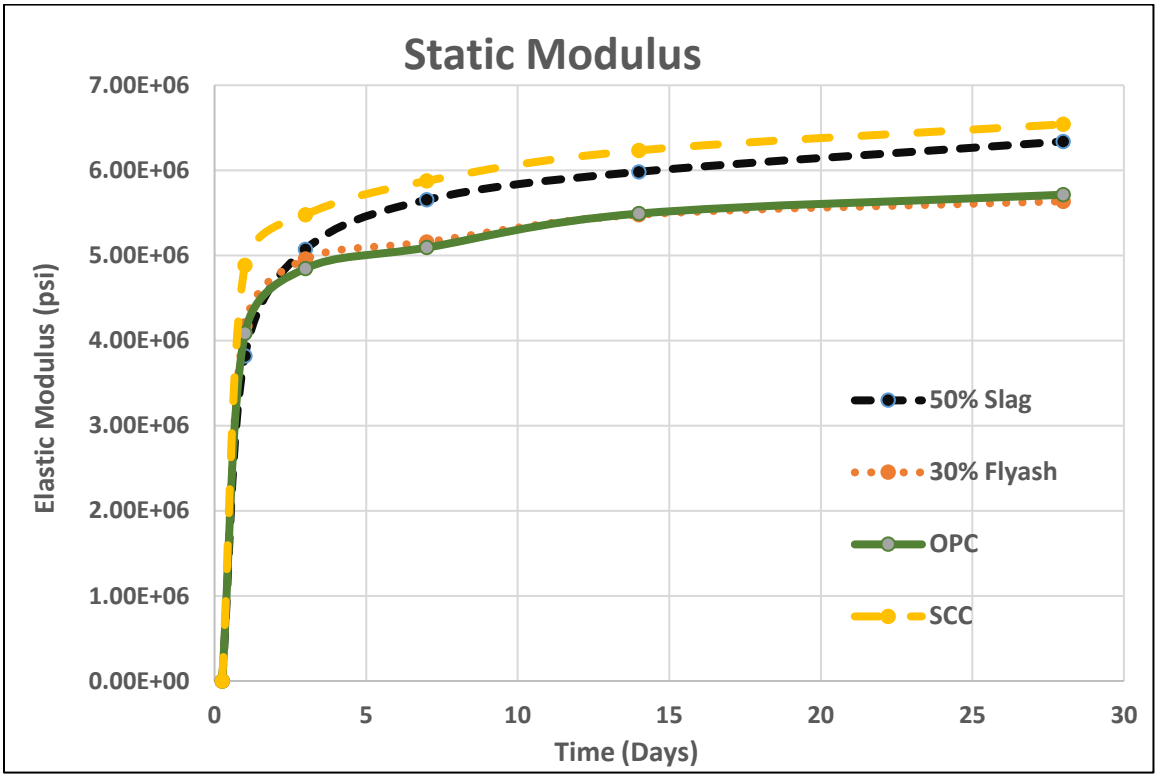

Figure 3-12 *– Relationship of Static Modulus of Elasticity and Age for Slag, Flyash, OPC, and SCC*

3.3.2.1 – Poisson's Ratio

Poisson's Ratio was calculated using the corresponding transverse strains associated with the loading. The equation for Poisson's Ratio can be seen in the following equation:

$$\nu = \frac{\epsilon_{t2} - \epsilon_{t1}}{\epsilon_{2-0.000050}}$$

Equation 3-3 *– Poisson's Ratio*

Where

- v = Poisson's Ratio

- ϵ_{t2} = Transverse strain at midheight of the specimen produced by stress S_2
- ϵ_{t1} = Transverse strain at midheight of the specimen produced by stress S_1
- ϵ_2 = Longitudinal strain produced by stress S_2

Calculated Poisson's Ratio for each of the concrete mixes is shown below in **Table 3-9**. In most cases, Poisson's ratio increases with concrete age. Each of the different concrete mixes has a calculated Poisson's ratio between the range of 0.14 – 0.18, indicating that the assumed value of 0.20 was slightly high.

Poisson's Ratio Comparison				
Test Day	**50% Slag**	**30% Flyash**	**OPC**	**SCC**
1	0.15	0.17	0.16	0.15
3	0.14	0.16	0.18	0.16
7	0.16	0.13	0.15	0.17
14	0.18	0.15	0.17	0.18
28	0.18	0.16	0.17	0.18

***Table 3-9** – Poisson's Ratio for Concrete Mixes*

3.3.3 – Ultrasonic Pulse Velocity Test

The goal of the Ultrasonic Pulse Velocity Method is to determine the travel time of ultrasonic pulse waves that pass through the concrete prism specimens. Based off these travel times, specimen dimensions, and weight, the Dynamic Modulus of Elasticity, E_d, can be calculated. As the concrete samples continue to age, the pulse wave travel time decreases, resulting in a faster wave velocity and a higher Dynamic Modulus.

3.3.3.1 – Test Procedure

For this experiment, two 3” x 4” x 16” rectangular prisms were used, in addition to one 6” x 12” cylindrical specimen. The Ultrasonic Pulse Velocity equipment consists of:

- Pulse Generator and Transmitting Transducer
- Receiving Transducer and Amplifier
- Time Measuring Circuit
- Bitscope Display Unit

Each of these components can be seen in the ASTM schematic in **Figure 3-13**. Details of the equipment and the setup are described in the ASTM Standard for “Standard Test Method for Pulse Velocity Through Concrete” (ASTM C597, 2009). The actual equipment and setup used in this research study can be seen in **Figure 3-14**, **Figure 3-15**, and **Figure 3-16**.

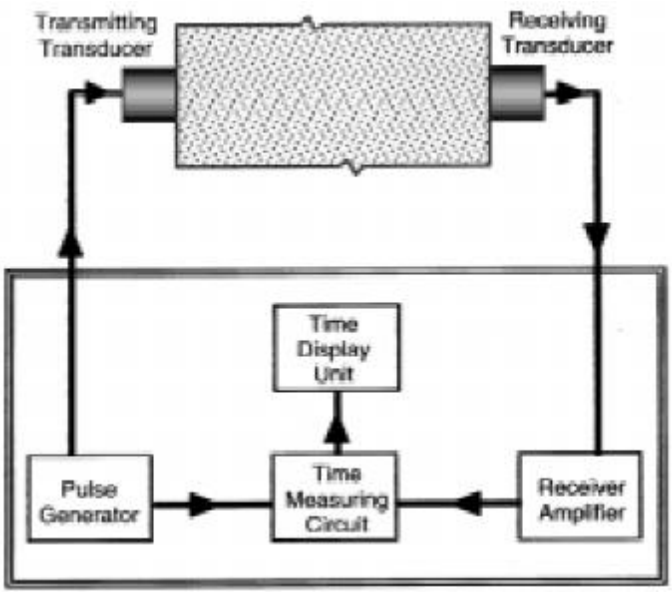

Figure 3-13 *– UPV Setup (ASTM C597, 2009).*

Figure 3-14 *– Pulse Generator and Broadband Receiver Amplifier*

Figure 3-15 *– Bitscope Data Acquisition System*

Figure 3-16 *– Pulsar Transmitting Transducer (Right) and Receiving Transducer (Left) and Coupling Agent*

The purpose of the test equipment is to develop a system with the ability to generate a pulse, transmit the pulse into one end of the concrete sample, and receive the pulse on the opposite side of the specimen. A coupling agent was used on the transducers to create a suitable medium between the transducers and the concrete specimen. The wave form of the pulse is then displayed on the Bitscope display unit for analysis.

Bitscope is a data acquisition software that must be downloaded on to a PC to conduct an analysis on the wave forms. Each time the transducers contact the specimen, the wave form is displayed on the computer screen as seen in **Figure 3-17**. The Bitscope application can capture, display, and record the analog waveforms, logic traces, frequency spectrum, and timing diagrams (Dashti, 2016). By adjusting various parameters available on the application, users can analyze measurements, frequencies, and wave speeds transmitted from the transducers through the specimens.

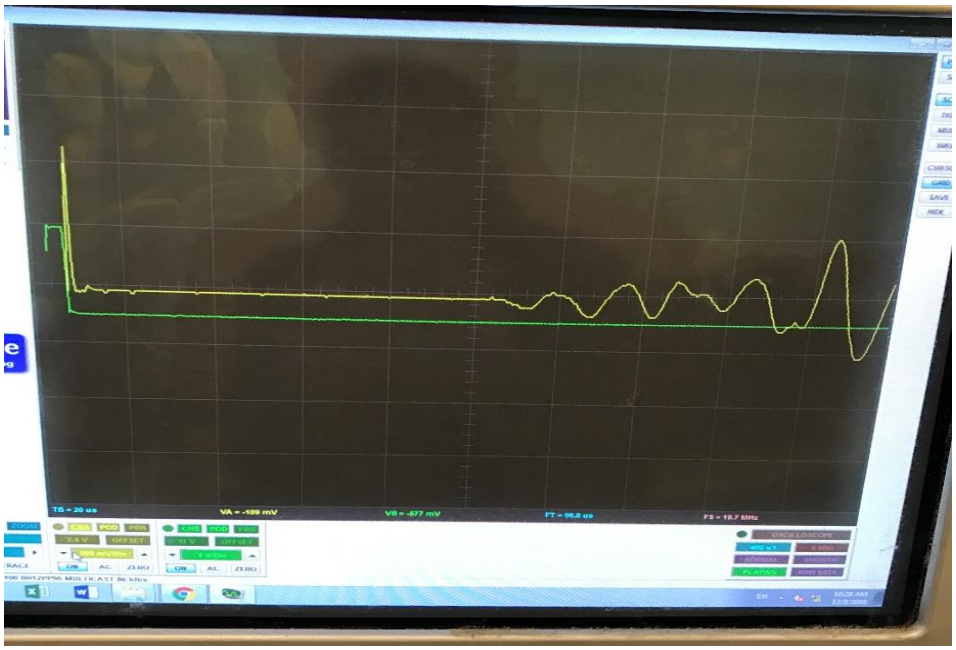

Figure 3-17 *– Bitscope Display Screen*

The wave travel time can be acquired by using the cursor function on the Bitscope display system, with the starting point at the highest peak at the beginning of the wave, and the ending point at the lowest point of the first sinusoidal curve. The time in-between these points represents the time it took for the pulse wave to travel from the pulsar transducer to the receiving transducer.

It is important to note that it takes approximate 1.9 microseconds for the receiving transducers to transform the analog waveforms into digital waveforms. Therefore, 1.9 microseconds were deducted from the travel time to obtain more accurate results.

3.3.3.2 – Results

The Dynamic Modulus equation is contingent on the mass density of the specimens, therefore each specimen was towel-dried, and weighed prior to conducting the analysis. The mass density of the specimens remained constant throughout the duration of the experiment. These mass densities were calculated from the specimen weights, which can be seen in **Table 3-10** below:

Specimen Density (pcf)			
50% Slag	**30% Flyash**	**OPC**	**SCC**
152.82	151.41	147.96	149.16

Table 3-10 *- Mass Densities for Concrete Specimens*

The boundary conditions were kept constant for the specimen, as outlined in the ASTM Standard for Pulse Velocity through concrete (ASTM C597, 2009). Each specimen underwent three UPV tests, and the travel times were averaged to ensure accuracy with the results. The resolution of the data is 0.2 µs. Once the travel times were obtained, the wave velocity was calculated by diving the length of the specimen by the wave travel time. The wave travel times and wave velocities for all four of the concrete mixes can be seen below in **Table 3-11**. As seen in the table, the wave velocity increases as the travel time decreases, and the concrete becomes more mature and strengthens. As the pulse velocity increases, it results in a higher Dynamic Modulus of Elasticity.

Travel Time and Wave Speed Comparison (Resolution = 0.2µs)								
Test Day	50% Slag		30% Flyash		OPC		SCC	
	Travel Time (µs)	Wave Speed (in./sec)	Travel Time (µs)	Wave Speed (in./sec)	Travel Time (µs)	Wave Speed (in./sec)	Travel Time (µs)	Wave Speed (in./sec)
1	94.4	155,378	93.4	153,127	92.8	158,119	84.4	168,009
3	91.4	174,052	86.8	164,207	85.8	170,862	80.2	177,580
7	83.4	179,760	85.2	168,219	83.2	176,058	78.2	182,579
14	82.0	182,927	83.6	171,382	82.6	177,643	77.6	184,687
28	80.6	186,017	82.8	173,589	80.8	181,249	76.0	188,458

Table 3-11 *– Ultrasonic Wave Travel Time and Wave Velocity Results*

A graphical representation of the Ultrasonic wave speed vs. time can be seen below in **Figure 3-18**. As seen, the Self-Consolidating Concrete mix yielded the highest wave velocity at all ages. Because each of the concrete batches had similar mass densities, the calculated Dynamic Modulus was proportionate, thus SCC would result in the greatest modulus. The 30% Flyash batch resulted in the lowest wave velocities at each age.

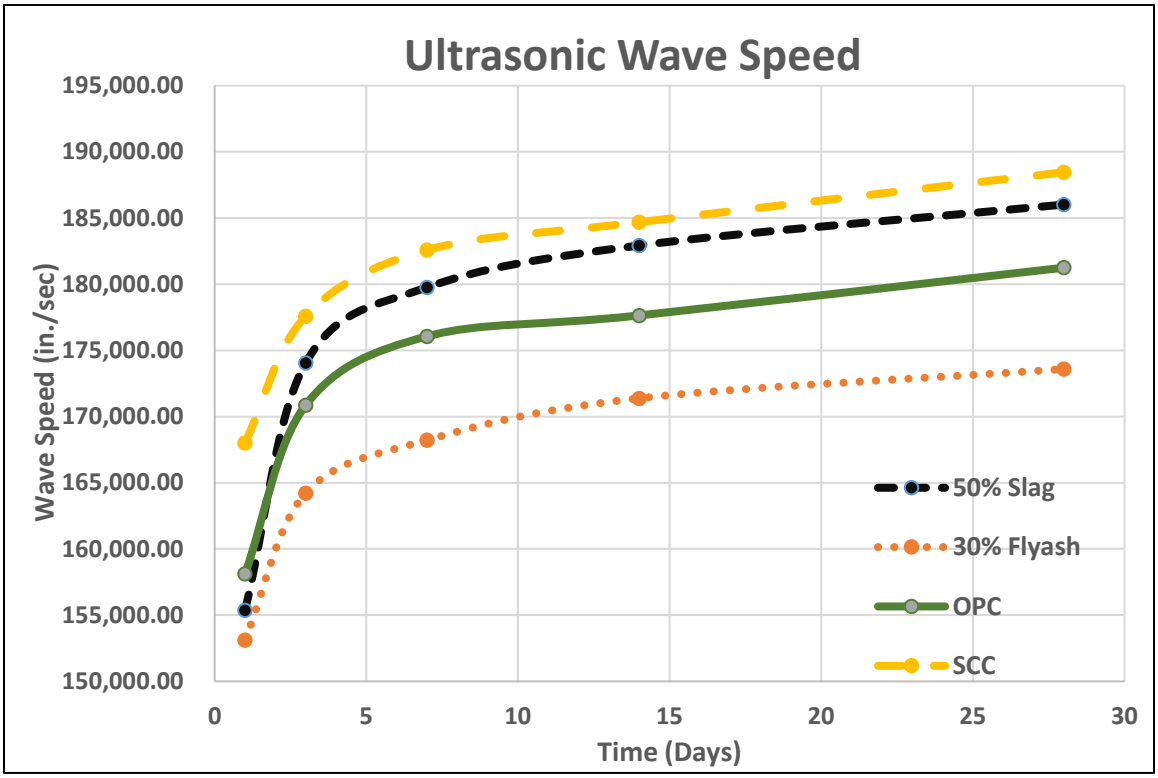

Figure 3-18 *– Ultrasonic Wave Speed vs. Time for Concrete Specimens*

After the wave velocities were determined, the Dynamic Modulus of Elasticity was calculated using the following equation:

$$E = \frac{V_P^2 \rho (1+v)(1-2v)}{(1-v)}$$

Equation 3-4 *– Dynamic Modulus from Pulse Velocity (Popovics, 2008).*

Where:

- E = Dynamic Modulus of Elasticity (psi)
- V_p = Ultrasonic Pulse Velocity (in/sec)
- ρ = mass density (slug/in^3)
- ν = Poisson's Ratio (Assumed 0.2 for All Samples)

From **Equation 3-4**, the calculated Dynamic Moduli based off ultrasonic pulse wave velocities for all four concrete mixes can be seen below in **Table 3-12**:

Dynamic Modulus Comparison - UPV (psi)				
Test Day	**50% Slag**	**30% Flyash**	**OPC**	**SCC**
1	4.97E+06	4.70E+06	4.97E+06	5.71E+06
3	6.17E+06	5.41E+06	5.79E+06	6.38E+06
7	6.59E+06	5.70E+06	6.15E+06	6.75E+06
14	6.80E+06	5.93E+06	6.28E+06	6.90E+06
28	7.05E+06	6.08E+06	6.53E+06	7.19E+06

***Table 3-12** – Dynamic Modulus from Ultrasonic Pulse Wave Velocity*

A graphical representation of the Dynamic Modulus with respect to concrete age can be seen in **Figure 3-19** below. It was determined the SCC resulted in the highest Dynamic Modulus, while the Flyash batch resulted in the lowest Dynamic Modulus, similar to the Static Modulus. The SCC and Slag batch were very close to converging at 28 days.

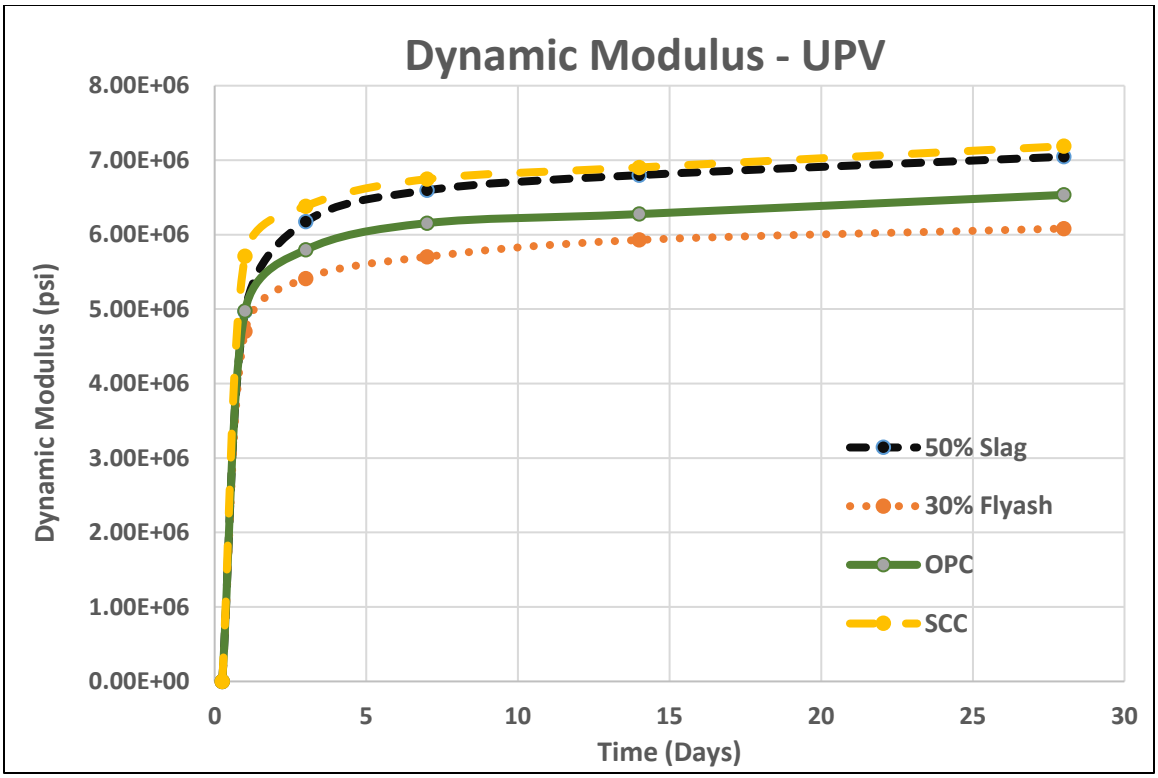

Figure 3-19 *– Dynamic Modulus from UPV vs. Time*

Poisson's Ratio can influence the Dynamic Modulus value. 0.20 was assumed for this experiment, however it was determined earlier that the actual Poisson's Ratio for the concrete samples varied from 0.14 – 0.19. A sensitivity analysis was conducted below in **Table 3-13** to determine the influence that different values of Poisson's Ratio would have on the Dynamic Modulus from UPV. As seen from the table, when Poisson's Ratio is reduced, the calculated modulus values are increased. When Poisson's Ratio is assumed at 0.15, E_{UPV} increases by approximately 0.35E6 psi.

Effect of Poisson's Ratio on E_{UPV} (psi) at 28 Day				
Poisson's Ratio	**50% Slag**	**30% Flyash**	**OPC**	**SCC**
0.15	7.41E+06	6.40E+06	6.88E+06	7.56E+06
0.16	7.35E+06	6.34E+06	6.82E+06	7.50E+06
0.17	7.28E+06	6.29E+06	6.75E+06	7.43E+06
0.18	7.21E+06	6.22E+06	6.69E+06	7.35E+06
0.19	7.13E+06	6.15E+06	6.61E+06	7.27E+06
0.2	**7.05E+06**	**6.08E+06**	**6.53E+06**	**7.19E+06**

Table 3-13 *– Effect of Poisson's Ratio on EPV after 28 Days*

The wave travel time and wave velocity for the 3" x 4" x 16" prisms were compared to the 6" x 12" cylindrical specimens. The results for each concrete mix can be seen in **Table 3-14** below. It is found that the cylindrical specimens produced a smaller wave velocity as compared to that of the rectangular prism specimens of the same concrete mix. This could be due to the quantity of data points that are displayed from the pulse velocity travel times. Shorter specimens, such as the cylinders, result in fewer data points, which result in lower accuracy. This could explain why the cylindrical specimens resulted in lower modulus values as well.

Wave Travel Time and Wave Speed - Slag				
Test Day	Prism		Cylinder	
	Travel Time (µs)	Wave Speed (in./sec)	Travel Time (µs)	Wave Speed (in./sec)
1	102.8	155,693	77.57	154,706
3	91.4	175,204	70.63	169,891
7	88.6	180,700	68.10	176,211
14	86.6	184,686	67.83	176,904
28	85.4	187,378	66.23	181,178

Wave Travel Time and Wave Speed - OPC				
Test Day	Prism		Cylinder	
	Travel Time (µs)	Wave Speed (in./sec)	Travel Time (µs)	Wave Speed (in./sec)
1	101.2	158,051	75.8	158,242
3	93.6	171,123	70.6	169,891
7	90.6	176,665	68.6	174,842
14	89.6	178,638	68.6	175,182
28	87.6	182,718	67.4	178,306

Wave Travel Time and Wave Speed - Flyash				
Test Day	Prism		Cylinder	
	Travel Time (µs)	Wave Speed (in./sec)	Travel Time (µs)	Wave Speed (in./sec)
1	101.8	157,119	76.4	157,137
3	93.4	171,367	73.8	162,382
7	91.8	174,102	71.8	167,364
14	90.2	177,449	70.4	170,535
28	89.8	178,372	69.0	173,829

Wave Travel Time and Wave Speed - SCC				
Test Day	Prism		Cylinder	
	Travel Time (µs)	Wave Speed (in./sec)	Travel Time (µs)	Wave Speed (in./sec)
1	95.2	168,008	73.6	163,117
3	90.2	177,580	70.2	171,184
7	87.6	182,579	68.8	174,165
14	86.6	184,686	68.2	175,695
28	84.8	188,457	67.2	178,483

Table 3-14 *– Wave Travel Time and Wave Velocity Comparison between Cylindrical Specimens and Rectangular Prison Specimens*

The comparison between the modulus values for the cylindrical and prism specimens can be seen below:

Dynamic Modulus (psi) - Slag			
Test Day	Prism	Cylinder	% Diff
1	5.02E+06	4.86E+06	3%
3	6.39E+06	5.86E+06	8%
7	6.79E+06	6.30E+06	7%
14	7.10E+06	6.35E+06	11%
28	7.30E+06	6.66E+06	9%

Dynamic Modulus (psi) - OPC			
Test Day	Prism	Cylinder	% Diff
1	4.98E+06	4.96E+06	1%
3	5.88E+06	5.62E+06	4%
7	6.25E+06	5.96E+06	5%
14	6.42E+06	5.99E+06	7%
28	6.70E+06	6.20E+06	7%

Dynamic Modulus (psi) - Flyash			
Test Day	Prism	Cylinder	% Diff
1	4.52E+06	4.89E+06	-8%
3	5.60E+06	5.22E+06	7%
7	5.84E+06	5.56E+06	5%
14	6.07E+06	5.79E+06	5%
28	6.15E+06	6.02E+06	2%

Dynamic Modulus (psi) - SCC			
Test Day	Prism	Cylinder	% Diff
1	5.71E+06	5.32E+06	7%
3	6.38E+06	5.85E+06	8%
7	6.75E+06	6.06E+06	10%
14	6.90E+06	6.17E+06	11%
28	7.19E+06	6.36E+06	11%

Table 3-15 *– Dynamic Modulus Comparison between Cylindrical Specimens and Rectangular Prism Specimens*

3.3.4 – Impact Resonance Frequency Test

In addition to determining the Dynamic Modulus of Elasticity from ultrasonic pulse velocities, E_d was also determined using the Impact Resonance Frequency Method. The goal of this method is to determine the fundamental resonant frequencies of the specimen. The specimen is supported by appropriate boundary conditions, and struck with an impact hammer. The response of the specimen is then measured by the accelerometer and recorded. Using

digital signal processing methods, the fundamental frequency of vibration can then be determined based on the location of the impact point and location of the accelerometer on the specimen (ASTM 215-08). As the concrete matures, the fundamental transverse frequency will increase, thus resulting in a higher Dynamic Modulus as the concrete specimen strengthens.

3.3.4.1 – Test Procedure

For this research study, two 3" x 4" x 16" rectangular prisms from each concrete mix were used. The Impact Resonance Frequency test equipment consists of:

- Impact Hamer
- Accelerometer
- Amplifier
- Data Acquisition System/Waveform Analyzer (LabVIEW)

The equipment used in this research study can be seen in **Figure 3-20**. The impact point was located in the direct center of the face of the prism, and the accelerometer location was centered 1.5" from the edge of the specimen. The accelerometer was attached to the specimen with a hot glue adhesive, and removed following each test. Locations of the accelerometer, impact point, and boundary conditions remained constant for each of the specimens from all of the concrete mixes.

Figure 3-20 *– Impact Hammer, Accelerometer, and Specimen used in Study*

For each test, the impact hammer struck the specimen three times, with approximately the same magnitude of force. The frequency vs. amplitude domain was then plotted on the LabVIEW waveform analyzer as see in **Figure 3-21**. The top plot of **Figure 3-21** shows the time graph of the impact i.e. the duration of the impact strike measured by the accelerometer. The middle graph shows the free vibration of the specimen after impact (not including vibrations due to impact). As seen in the bottom plot, the frequency response function is generated through Fast Fourier Transform. The frequency domain is plotted against the amplitude. All data points are generated on a text file, and were then be plotted on excel. The resonance frequencies from the impact were then determined by finding the frequency that correlates to

the maximum amplitude. Each resonance frequency was determined for the impacts on each specimen.

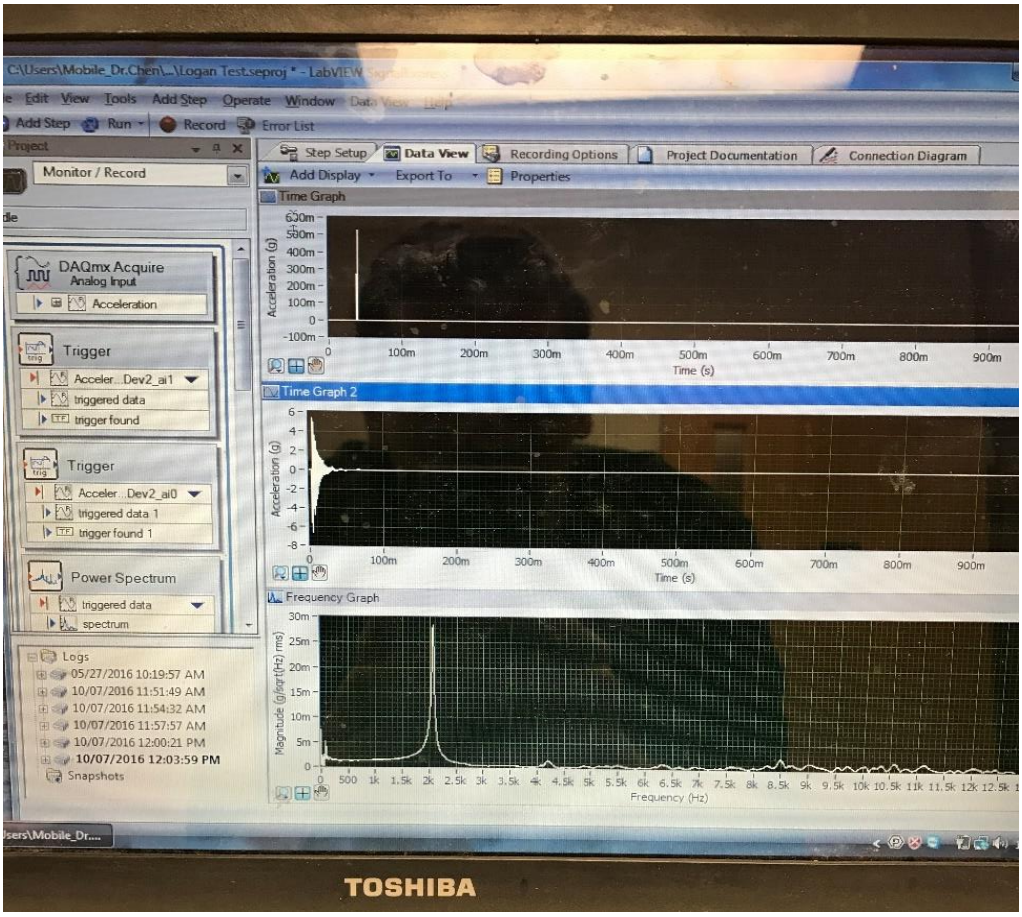

Figure 3-21 *– LabVIEW Waveform Analyzer*

3.3.4.1 – Results

The Dynamic Modulus calculated from resonance frequencies is contingent on the mass density and the dimensions of the specimens. Each specimen was towel dried to eliminate excess water, and weighed prior to each test to maintain accuracy. The impact resonance frequency method was not conducted on the 50% slag specimens until the day 7 test. All other

specimens underwent the test on days 1,3,7,14 and 28. Each specimen underwent at least three impact strikes, and the transverse resonance frequencies were determined as followed:

Transverse Frequency Comparison (Hz)				
Test Day	**50% Slag**	**30% Flyash**	**OPC**	**SCC**
1		1,913	1,875	2,056
3		2,123	2,055	2,191
7	2,161	2,170	2,124	2,251
14	2,188	2,199	2,165	2,290
28	2,262	2,224	2,195	2,320

Table 3-16 *– Transverse Resonance Frequency Results (Resolution = 1Hz)*

As seen, the Self-Consolidating Concrete mix yielded the highest transverse frequencies at all ages, thus resulting in an overall higher modulus given that the weights/densities were similar for all four concrete batches. ASTM provides the equation that is used to calculate the Dynamic Modulus which was also derived earlier:

$$E_d = CMn^2$$

Equation 3-5 *– Dynamic Modulus from Transverse Resonance Frequencies (ASTM C215-08)*

Where:

$$C = 0.9464\ \frac{L^3T}{bt^3}$$

Equation 3-6 *– Factor based on Geometry of Specimen and Mode of Vibration*

- C = 0.9464 (L^3T/bt^3) (in^{-1})
- M = Mass of the specimen (slugs)
- n = Fundamental Transverse Frequency (Hz)
- L = Length of Specimen (16 in.)

- t,b = Dimensions of Cross section of Prism (3,4 in.)
- T = Correction Factor that depends of the Ratio of the Radius of Gyration, K (t/3.464 for Prism) and the Length, L of the specimen. See **Table 3-17**

As mentioned earlier in the literature review section, ASTM C215-08 gives a table that can be used to determine the correction factor T, based on K/L value from the specimen dimensions, and the assumed Poisson's Ratio of the mix.

K/L	Value of T[A]			
	μ = 0.17	μ = 0.20	μ = 0.23	μ = 0.26
0.00	1.00	1.00	1.00	1.00
0.01	1.01	1.01	1.01	1.01
0.02	1.03	1.03	1.03	1.03
0.03	1.07	1.07	1.07	1.07
0.04	1.13	1.13	1.13	1.14
0.05	1.20	1.20	1.21	1.21
0.06	1.28	1.28	1.29	1.29
0.07	1.38	1.38	1.39	1.39
0.08	1.48	1.49	1.49	1.50
0.09	1.60	1.61	1.61	1.62
0.10	1.73	1.74	1.75	1.76
0.12	2.03	2.04	2.05	2.07
0.14	2.36	2.38	2.39	2.41
0.16	2.73	2.75	2.77	2.80
0.18	3.14	3.17	3.19	3.22
0.20	3.58	3.61	3.65	3.69
0.25	4.78	4.84	4.89	4.96
0.30	6.07	6.15	6.24	6.34

***Table 3-17** –Values of Correction Factor, T (ASTM C215-08)*

K/L was determined to be 0.072 for the rectangular prisms. Linear interpolation was used to solve for T = 1.3884. With the use of the ASTM equation and the above-mentioned correction factor, the Dynamic Modulus for each of the four concrete samples was calculated and can be seen in **Table 3-18** below:

Dynamic Modulus Comparison - Impact (psi)				
Test Day	**50% Slag**	**30% Flyash**	**OPC**	**SCC**
1		3.86E+06	4.24E+06	5.18E+06
3		5.07E+06	5.11E+06	5.88E+06
7	5.97E+06	5.36E+06	5.47E+06	6.20E+06
14	6.12E+06	5.49E+06	5.69E+06	6.42E+06
28	6.54E+06	5.64E+06	5.85E+06	6.58E+06

Table 3-18 *– Dynamic Modulus from Impact Resonance Frequencies*

A graphical representation of the calculated Dynamic Moduli with concrete age can be seen in **Figure 3-22**. Similar to the calculated values from the UPV method, and the Static Modulus method, the SCC batch yielded the highest modulus at all ages, while flyash resulted in the lowest modulus. Similar to the Dynamic Modulus calculated from the UPV method, the Slag batch was close to converging to the SCC batch strength at 28 days.

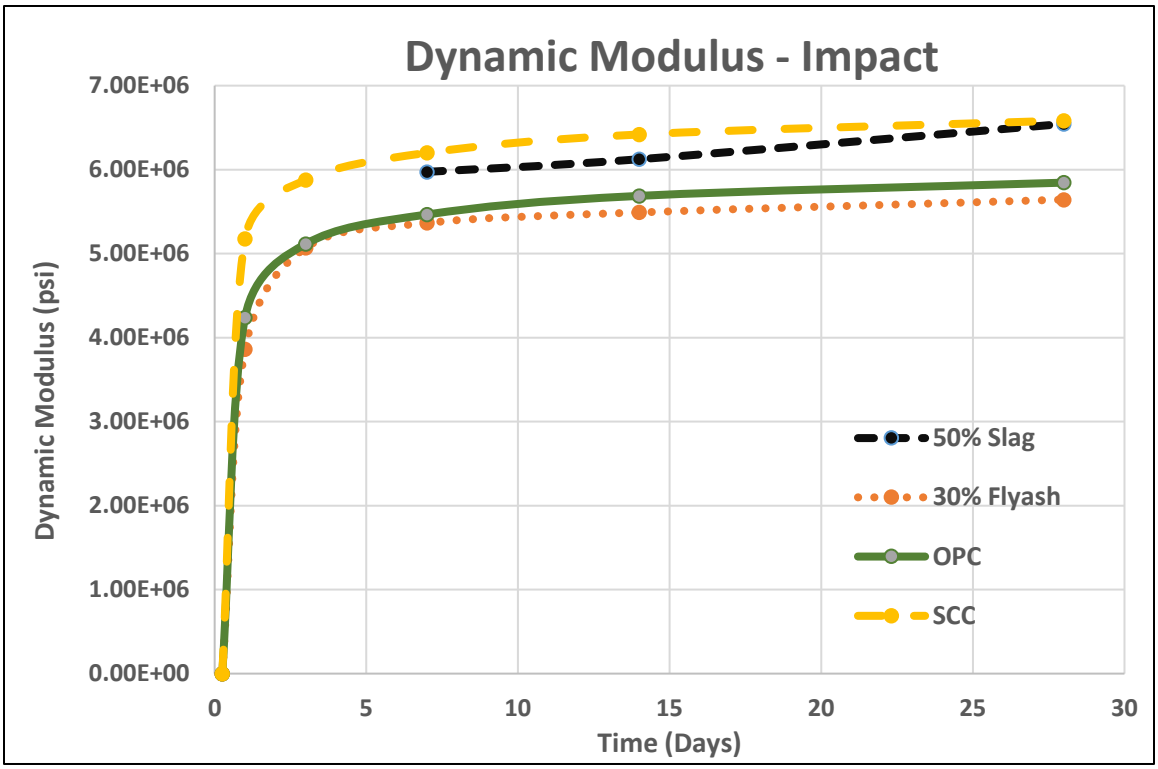

Figure 3-22 *– Dynamic Modulus vs. Age from Impact Resonance Frequencies*

Chapter 4 Analysis and Interpretation of Results

4.1 – Relationship of Static and Dynamic Modulus of Elasticity

One of the goals of this research study was to determine the relationship between the Static Modulus of Elasticity and the Dynamic Modulus of Elasticity in various types of common concrete mixes. This section will discuss the relationship of these modulus values for each of the different mixes.

4.1.1 – 50% Slag Batch

For the 50% Slag concrete batch, the Static Modulus, Dynamic Modulus via UPV, and Dynamic Modulus via vibration resonance frequencies were all calculated as described in earlier sections. The calculated moduli values can be seen in **Table 4-1**. **Figure 4-1** shows the graphical representation of the relationship of these values with concrete age. As noted earlier, the vibration resonance frequency method was only conducted on 7, 14 and 28 days.

50% Slag Batch (psi)			
Day	**Static Modulus**	**Dynamic Modulus - UPV**	**Dynamic Modulus - Impact Hammer**
1	3.82E+06	4.97E+06	
3	5.07E+06	6.17E+06	
7	5.65E+06	6.59E+06	5.97E+06
14	5.98E+06	6.80E+06	6.12E+06
28	6.34E+06	7.05E+06	6.54E+06

***Table 4-1** – Static and Dynamic Modulus for 50% Slag Concrete Mix*

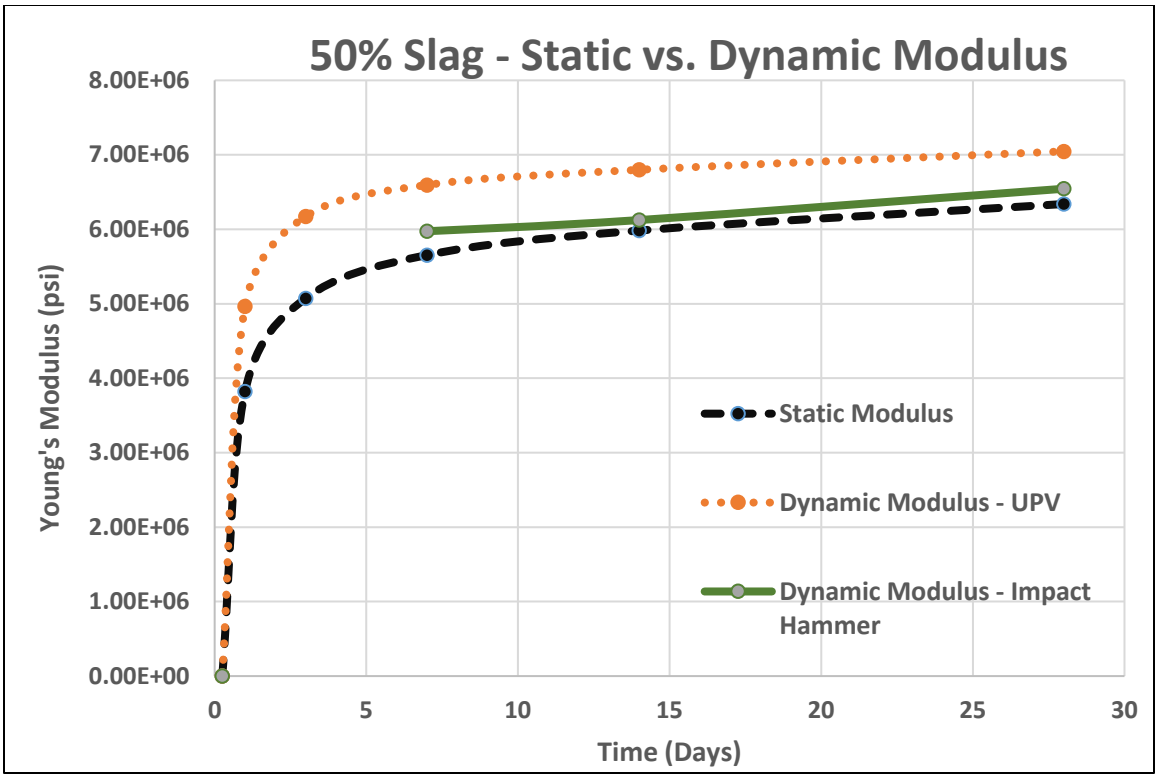

Figure 4-1 *– Relationship Between Static and Dynamic Modulus for 50% Slag*

As seen in the table and graph, the UPV method to determine the Dynamic Modulus clearly resulted in the highest value at all ages. The calculated Static Modulus was the lowest of the three, while the vibration resonance method resulted in a modulus value slightly higher than the Static Modulus. The ratios of the three methods were calculated at each testing age, and are shown below in **Table 4-2**:

50% Slag			
Day	**E/E_{UPV}**	**E/E_{impact}**	**E_{impact}/E_{UPV}**
1	0.769		
3	0.822		
7	0.857	0.946	0.906
14	0.880	0.977	0.901
28	0.900	0.969	0.929

***Table 4-2** – Ratios for E, E_{UPV} and E_{Impact} for 50% Slag Mix*

As seen in the table, the ratio between E and E_{UPV} became closer to one with the concrete age. The 28-day Static Modulus was approximately 90% of the Dynamic Modulus from the UPV method. The Static Modulus and the Dynamic Modulus from resonance frequencies were almost identical to each other at each testing date. E_{UPV} was approximately 9% greater than E_{impact} at each testing age.

4.1.2 – 30% Flyash Batch

The same analysis was conducted for the 30% Flyash concrete mix. Each of the experiments were conducted on all testing ages. The calculated Modulus values obtained from the three experimental procedures can be seen below in **Table 4-3**: **Figure 4-2** shows the relationship of these values with the concrete age.

30% Flyash Batch (psi)			
Day	Static Modulus	Dynamic Modulus - UPV	Dynamic Modulus - Impact Hammer
1	4.17E+06	4.70E+06	3.86E+06
3	4.96E+06	5.41E+06	5.07E+06
7	5.16E+06	5.70E+06	5.36E+06
14	5.48E+06	5.93E+06	5.49E+06
28	5.64E+06	6.08E+06	5.64E+06

Table 4-3 *– Static and Dynamic Modulus for 30% Flyash Concrete Mix*

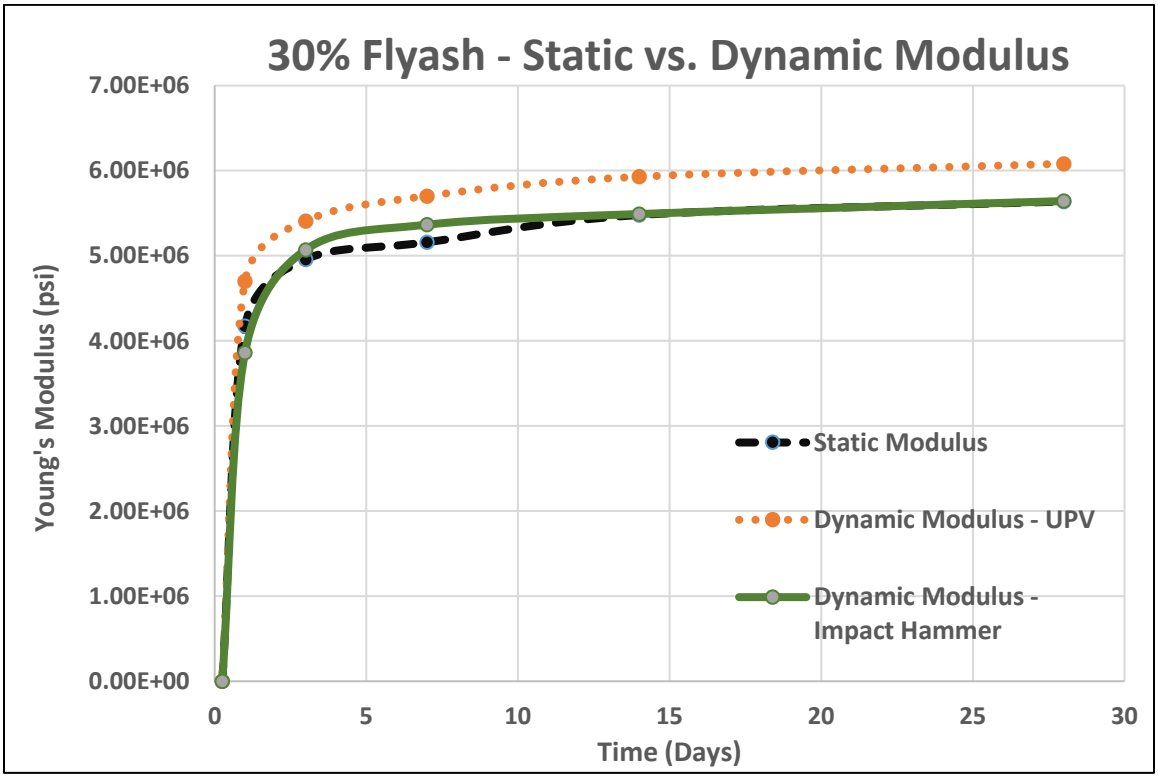

Figure 4-2 *– Relationship Between Static and Dynamic Modulus of 30% Flyash*

Similar to the 50% Slag mix, the UPV method resulted in the overall highest modulus. The Static Modulus was slightly lower than the impact hammer modulus value, however, they converged at 28 days. The ratios of the testing methods for the 30% flyash batch were calculated, and shown below in **Table 4-4**:

30% Flyash Batch			
Day	**E/E_{UPV}**	**E/E_{impact}**	**E_{impact}/E_{UPV}**
1	0.888	1.081	0.821
3	0.916	0.978	0.937
7	0.905	0.961	0.941
14	0.924	0.998	0.926
28	0.927	0.999	0.928

***Table 4-4** - Ratios for E, E_{UPV} and E_{Impact} for 30% Flyash Mix*

As seen in the table, the ratio between Dynamic Modulus from UPV and the Static Modulus became closer to 1 with concrete age. At 28 days, E/E_{UPV} was approximately 93%. The impact hammer method and the Static Modulus method produced very similar values at all ages. E_{UPV} was approximately 7% greater than E_{impact} at each testing age after three days.

4.1.3 – OPC Batch

The three experimental procedures were all conducted on the OPC concrete mix for each testing age. The calculated modulus values can be seen in **Table 4-5**. **Figure 4-3** shows the relationship between these moduli and concrete age for the OPC batch.

OPC Batch (psi)			
Day	**Static Modulus**	**Dynamic Modulus - UPV**	**Dynamic Modulus - Impact Hammer**
1	4.08E+06	4.97E+06	4.24E+06
3	4.85E+06	5.79E+06	5.11E+06
7	5.09E+06	6.15E+06	5.47E+06
15	5.49E+06	6.28E+06	5.69E+06
28	5.71E+06	6.53E+06	5.85E+06

***Table 4-5** – Static and Dynamic Modulus for OPC Concrete Mix*

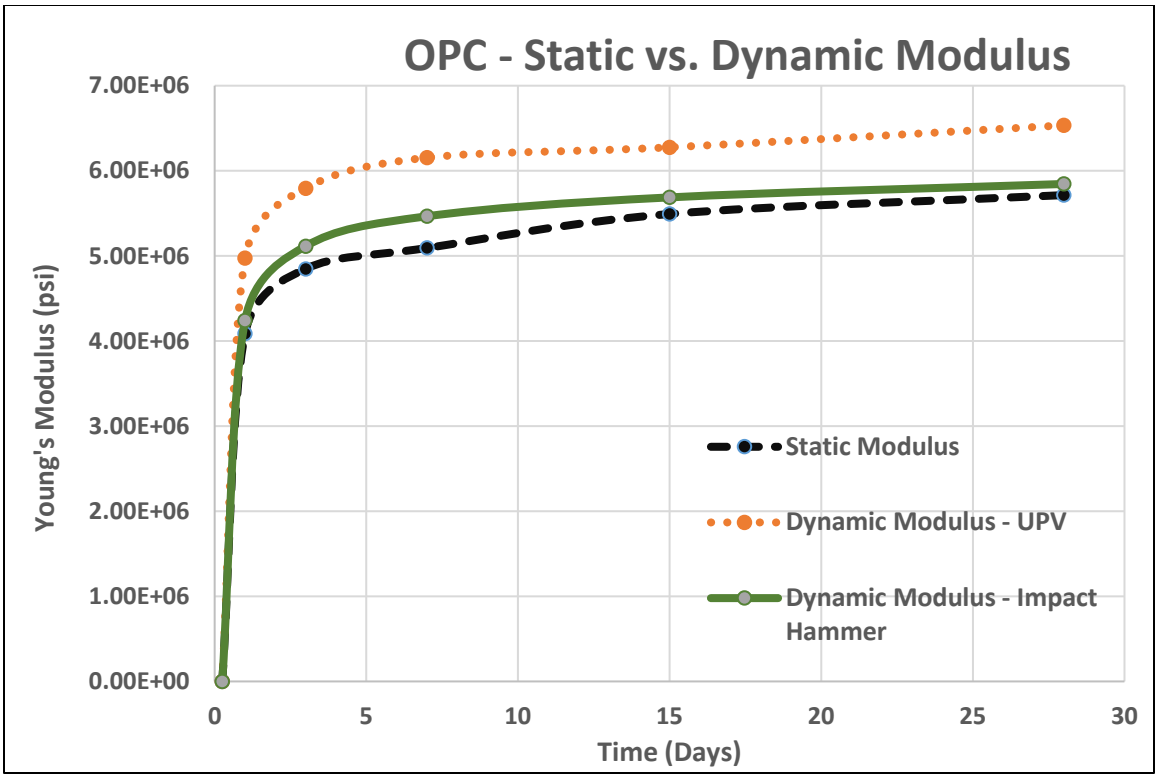

Figure 4-3 *– Relationship Between Static and Dynamic Modulus of OPC*

The OPC mix displayed results similar to both the slag and flyash mixes. The UPV method resulted in the highest modulus value at each testing age. The Static Modulus was the smallest of the three for each age. There was a larger difference between E_{Impact} and E than seen in the previous concrete mixes. The calculated ratios for the OPC mix are in **Table 4-6** below:

OPC Batch			
Day	**E/E_{UPV}**	**E/E_{impact}**	**E_{impact}/E_{UPV}**
1	0.821	0.964	0.852
3	0.836	0.948	0.883
7	0.828	0.932	0.888
14	0.875	0.966	0.906
28	0.875	0.978	0.895

Table 4-6 *- Ratios for E, E_{UPV} and E_{Impact} for OPC Mix*

As seen in the table, at 28 days, E/E_{UPV} was approximately 88%. The ratio between E and E_{impact} became closer to one with age, indicating that the modulus values were fairly similar to each other. E_{UPV} was approximately 10% greater than E_{impact} at each testing age.

4.1.4 – SCC Batch

The results from the three experimental procedures conducted on the Self-Consolidating Concrete mix are displayed in **Table 4-7** below. The graphical representation of the relationship between the three moduli value and concrete age can be seen in **Figure 4-4**.

SCC Batch (psi)			
Day	**Static Modulus**	**Dynamic Modulus - UPV**	**Dynamic Modulus - Impact Hammer**
1	4.88E+06	5.71E+06	5.18E+06
3	5.48E+06	6.38E+06	5.88E+06
7	5.88E+06	6.75E+06	6.20E+06
14	6.23E+06	6.90E+06	6.42E+06
28	6.54E+06	7.19E+06	6.58E+06

***Table 4-7** – Static and Dynamic Modulus for SCC Mix*

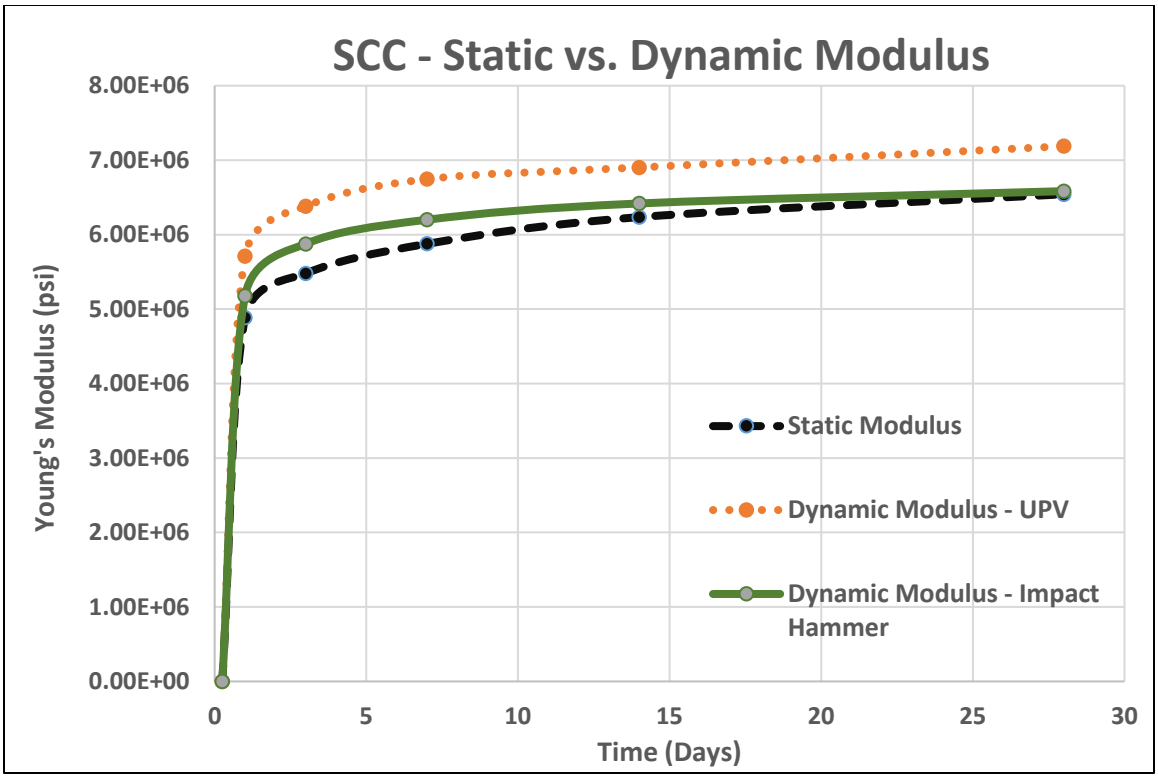

***Figure 4-4** – Relationship Between Static and Dynamic Modulus of SCC*

Similar to the previous three batches, the SCC batch produced similar relationships. The UPV method resulted in the highest modulus, while the Static Modulus was the smallest. It can also be seen that at later ages, the Static Modulus and the Modulus calculated from the impact method begin to converge. This was also seen in the previous three batches. The calculated ratios for the SCC mix are in **Table 4-8** below:

SCC Batch			
Day	**E/E_{UPV}**	**E/E_{impact}**	**E_{impact}/E_{UPV}**
1	0.855	0.944	0.906
3	0.859	0.932	0.921
7	0.871	0.948	0.919
14	0.903	0.971	0.930
28	0.910	0.994	0.916

***Table 4-8** - Ratios for E, E_{UPV} and E_{Impact} for SCC Mix*

As seen in the table, at 28 days, E/E_{UPV} was approximately 91%. The ratio between E and E_{impact} became closer to one with age, indicating that the modulus values were fairly similar to each other, especially at later ages. E_{UPV} was approximately 7-9% greater than E_{impact} at various testing ages.

4.2 – Correlation Between Modulus Testing Methods

In addition to determining the relationship between the Static and Dynamic Modulus for each of the four concrete mixes, the overall correlation between the three modulus testing methods was determined to develop an empirical relationship between them for any type of concrete. The relationship between the Static Modulus and Dynamic Modulus from the UPV Method (E and E_{UPV}) was analyzed. The relationship between the Static Modulus and the Dynamic Modulus from the impact hammer method (E and E_{impact}) was analyzed. Lastly, the relationship between the two methods of determining the Dynamic Modulus (E_{UPV} and E_{impact}) was analyzed. Empirical equations were developed based on the correlations of the methods, and the overall relationships were analyzed.

4.2.1 – Static and Dynamic (UPV)

For this analysis, the Static Modulus for all specimens of each concrete mix was plotted on excel on the x-axis, against the Dynamic Modulus (UPV method) on the y-axis. A trend line was inserted that best related values of the two methods starting at the origin. An equation of the trend line and the R^2 value of the trend line were generated. The graph of this correlation is seen below in **Figure 4-5**:

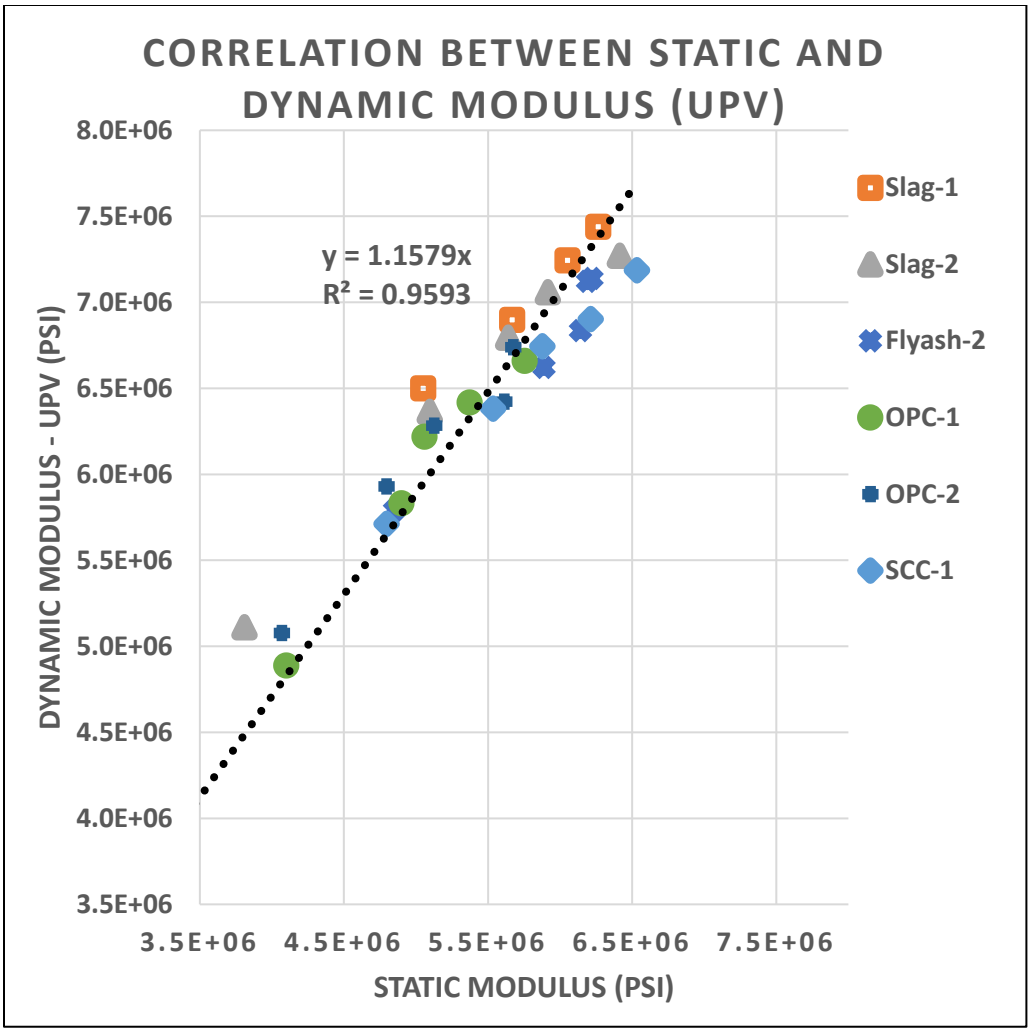

Figure 4-5 *– Correlation Between Static and Dynamic Modulus (UPV)*

It is seen that the relationship between E and E_{UPV} is linear, which is similar to what was found in previous research and literature review. The R^2 value is **0.9593**, which is close to 1. This indicates that the data is very close to the fitted regression line, and there is very little variability. From this data, the following empirical equation was determined, and can be used to estimate E_{UPV} from the Static Modulus, E, in psi:

$$E_{UPV} = 1.16E$$

***Equation 4-1** – Dynamic Modulus (E_{UPV}) from Static Modulus, E*

From this equation, it can be estimated that E_{UPV} is approximately 16% greater than the Static Modulus, E, based on the analysis of four different concrete batches.

4.2.2 – Static and Dynamic (Impact)

The same analysis was conducted to compare the relationship between the Static Modulus, and the Dynamic Modulus determined from impact hammer vibration frequencies. The Static Modulus for all specimens was plotted on the x-axis, against the Dynamic Modulus (Impact Method) on the y-axis starting at the origin. The results from this analysis are below in **Figure 4-6**:

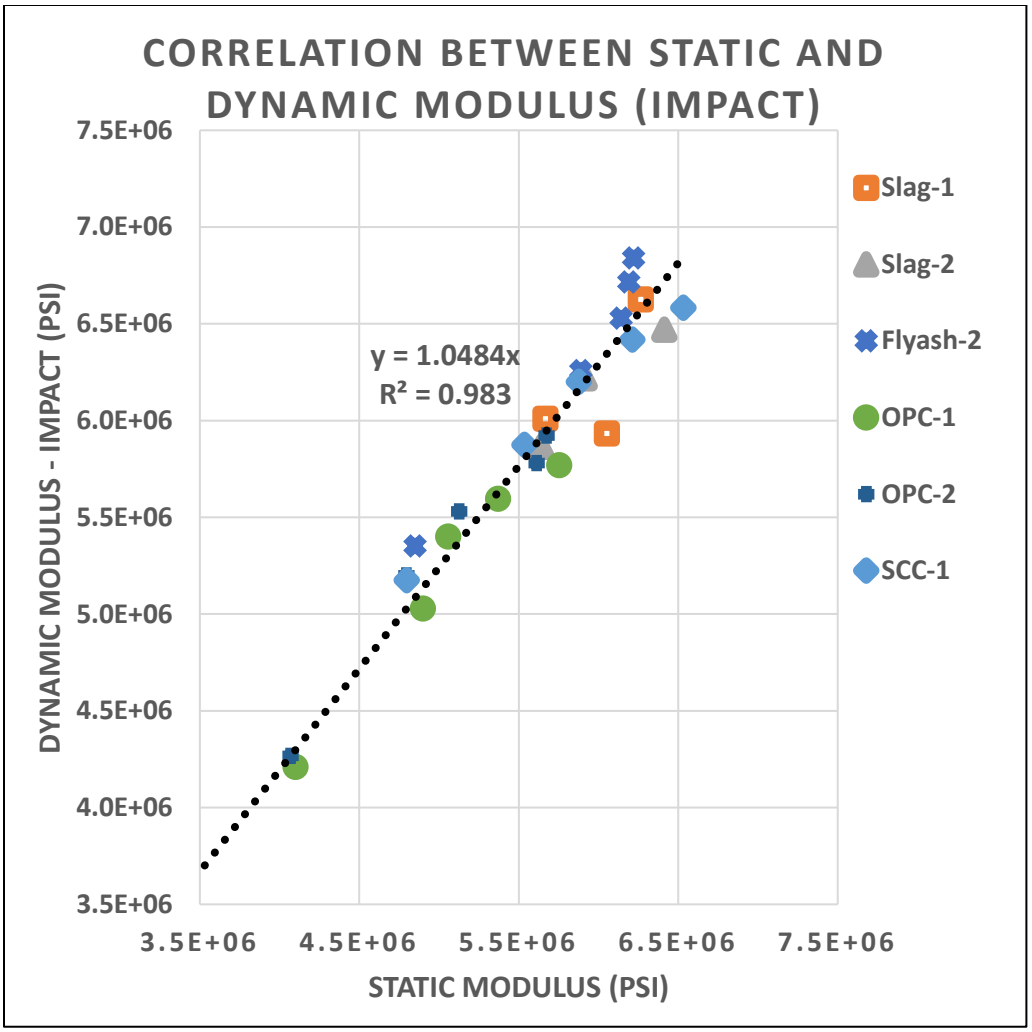

Figure 4-6 *– Correlation Between Static and Dynamic Modulus (Impact)*

It is seen that the relationship E and E_{impact} is also linear. The R^2 value for this analysis is **0.983,** indicating a very strong linear relationship between the two testing methods. From this data, the following equation was generated to estimate E_{impact} from the Static Modulus, E, in psi:

$$E_{Impact} = 1.05E$$

Equation 4-2 *– Dynamic Modulus (E_{Impact}) from Static Modulus, E*

From this equation, it can be estimated that E_{impact} is approximately 5% greater than the Static Modulus, E.

4.2.3 – Dynamic (UPV) and Dynamic (Impact)

In addition to relating the Static Modulus to the Dynamic Modulus, the two methods used to determine the Dynamic Modulus were also analyzed. The Dynamic Modulus (Impact) for all specimens was plotted on the x-axis against the Dynamic Modulus (UPV) on the y-axis. The graphical representation of this analysis is below in **Figure 4-7**:

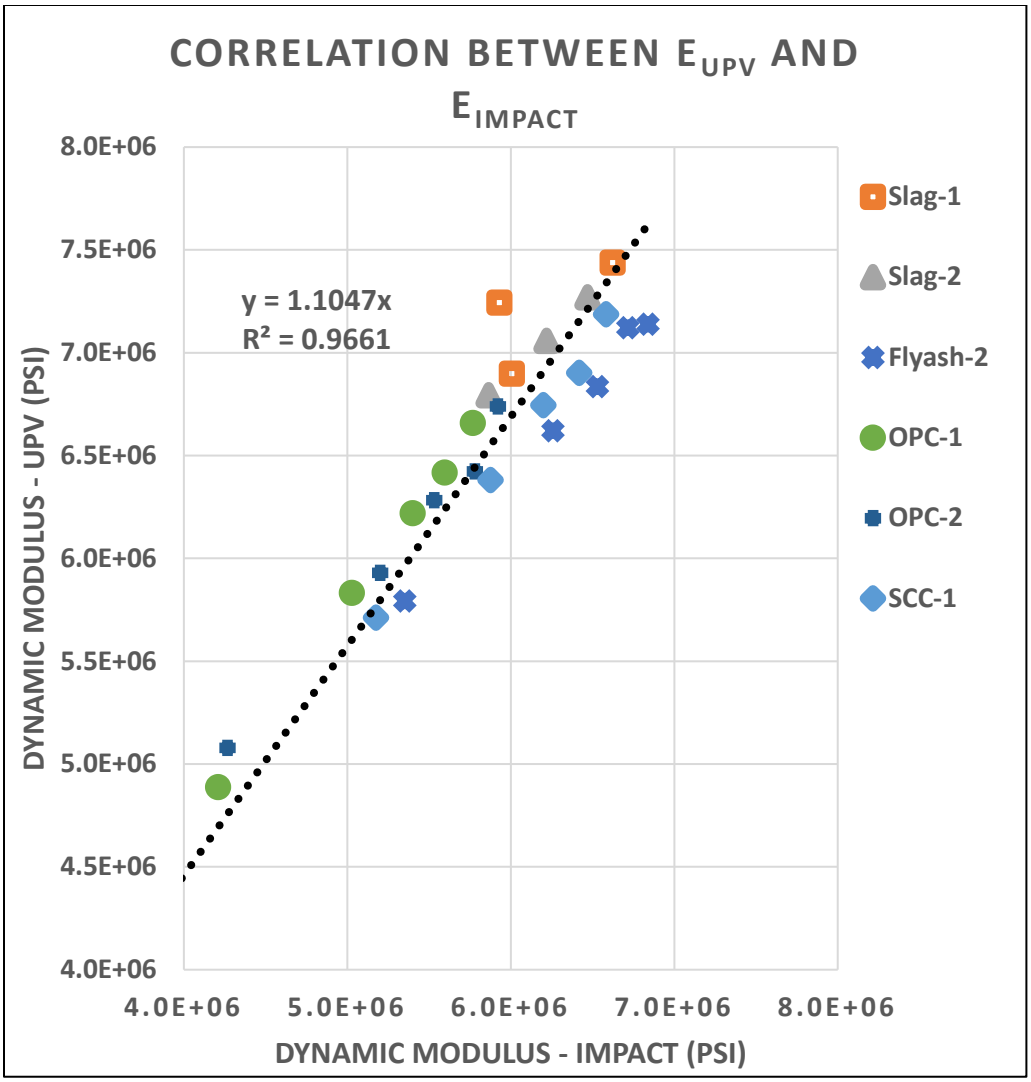

Figure 4-7 *– Correlation Between E_{UPV} and E_{Impact}*

It is seen from this figure that the relationship between calculated Dynamic Modulus values from the two methods is linear, with an R^2 value of **.9661**, indicating little variability of data from the trend line. The following equation was generated to estimate E_{UPV} from E_{Impact}:

$$E_{UPV} = 1.10E_{Impact}$$

Equation 4-3 *– Dynamic Modulus (E_{UPV}) from Dynamic Modulus (E_{Impact})*

From this equation, it can be estimated that E_{UPV} is approximately 10% greater than E_{Impact}.

4.2.4 – Correlation of Modulus Values at Early vs. Later Age

The data plotted in the previous figures contained all sample data from all ages of testing. Therefore, the equations of the linear trendlines were based on the average correlation between modulus values at all ages. The same analysis was conducted with the data, however any data after day 3 was excluded (Day 1 and Day 3 only). This would show how the empirical equations changed for early age concrete. The following equations were produced from data.

$$E_{UPV} = 1.21E$$

Equation 4-4 *– Dynamic Modulus (E_{UPV}) from Static Modulus (E) at Early Age*

$$E_{Impact} = 1.06E$$

Equation 4-5 *– Dynamic Modulus (E_{Impact})from Static Modulus (E) at Early Age*

$$E_{UPV} = 1.12E_{Impact}$$

Equation 4-6 *– Dynamic Modulus (E_{UPV}) from Dynamic Modulus (E_{Impact}) at Early Age*

As seen from the three equations, the difference between the calculated modulus values are greater at early ages i.e. greater separations between values.

The same analysis was conducted for late age concrete, in which only 28-day data was used. This analysis produced the following equations:

$$E_{UPV} = 1.14E$$

Equation 4-7 *- Dynamic Modulus (E_{UPV}) from Static Modulus (E) at 28 Days*

$$E_{Impact} = 1.03E$$

Equation 4-8 *- Dynamic Modulus (E_{Impact})from Static Modulus (E) at 28 Days*

$$E_{UPV} = 1.09E_{Impact}$$

***Equation 4-9** - Dynamic Modulus (E_{UPV}) from Dynamic Modulus (E_{Impact}) at 28 Days*

As seen from these three equations, the difference between the calculated modulus values are smaller at 28 days. **Table 4-9** shows how the correlation between modulus values changes based on concrete age.

Correlation at Different Concrete Age			
		E	**E_{Impact}**
Any Age	**E_{UPV}**	1.16 (R^2 = 0.9593)	1.10 (R^2 = 0.9661)
	E_{Impact}	1.05 (R^2 = 0.9830)	
Early Age	**E_{UPV}**	1.21 (R^2 = 0.9752)	1.12 (R^2 = 0.9876)
	E_{Impact}	1.06 (R^2 = 0.9925)	
28 Day	**E_{UPV}**	1.14 (R^2 = 0.9950)	1.09 (R^2 = 0.9924)
	E_{Impact}	1.03 (R^2 = 0.9959)	

***Table 4-9** – Correlation of Modulus Values at Different Concrete Ages*

As shown from the table and previous equations, the modulus values begin to converge upon each other as the concrete matures. It is also seen that the R^2 values increase with age as well, indicating that the linear relationship between modulus values strengthens with age.

4.3 – Relationship Between Compressive Strength and Young's Modulus

4.3.1 – ACI Equations

ACI provides several equations that are used to estimate Young's Modulus based on the 28-day compressive strength of the concrete specimens. It has typically been seen that the obtained E values are conservative when compared to E values obtained from the Static

Modulus Test. The first equation is based on the compressive strength and the density of the concrete.

$$E = 33 w_c^{1.5} \sqrt{f_c'}$$

Equation 4-10 *– Elastic Modulus from Compressive Strength and Density (ACI 318)*

Where:

- f_c' = 28-day compressive strength (psi)
- w_c = Density of concrete (lb/ft^3)

If normal-weight concrete is used, Equation 20 reduces to the following equation:

$$E = 57000 \sqrt{f_c'}$$

Equation 4-11 *– Elastic Modulus from Compressive Strength for Normal-Weight Concrete (ACI 318)*

4.3.2 – Relationships/Analysis

The obtained Modulus values from the Static experiment, and the ACI 318 equation based on concrete density were calculated, and can be seen below in **Table 4-10**:

50% Slag					
Age	**Compressive Strength (psi)**	**E (Static) (psi)**	**Unit Weight (lb/ft^3)**	**E (psi) ACI 318)**	**Error %**
1	1,345	3.82E+06	152.82	2.29E+06	40%
3	3,310	5.07E+06	152.82	3.59E+06	29%
7	4,854	5.65E+06	152.82	4.34E+06	23%
14	6,108	5.98E+06	152.82	4.87E+06	19%
28	6,605	6.34E+06	152.82	5.07E+06	20%
30% Flyash					
Age	**Compressive Strength (psi)**	**E (Static) (psi)**	**Unit Weight (lb/ft^3)**	**E (psi) ACI 318**	**Error %**
1	1,890	4.17E+06	156.96	2.82E+06	32%
3	3,657	4.96E+06	156.96	3.92E+06	21%
7	4,297	5.16E+06	156.96	4.25E+06	18%
14	4,695	5.48E+06	156.96	4.45E+06	19%
28	4,755	5.64E+06	156.96	4.47E+06	21%
OPC					
Age	**Compressive Strength (psi)**	**E (Static) (psi)**	**Unit Weight (lb/ft^3)**	**E (psi) ACI 318**	**Error %**
1	1,850	4.08E+06	149.76	2.60E+06	36%
3	3,462	4.85E+06	149.76	3.56E+06	27%
7	4,218	5.09E+06	149.76	3.93E+06	23%
14	4,974	5.49E+06	149.76	4.27E+06	22%
28	5,491	5.71E+06	149.76	4.48E+06	22%
SCC					
Age	**Compressive Strength (psi)**	**E (Static) (psi)**	**Unit Weight (lb/ft^3)**	**E (psi) ACI 318**	**Error %**
1	4,417	4.88E+06	150.12	4.03E+06	17%
3	6,704	5.48E+06	150.12	4.97E+06	9%
7	8,316	5.88E+06	150.12	5.54E+06	6%
14	9,311	6.23E+06	150.12	5.86E+06	6%
28	10,584	6.54E+06	150.12	6.24E+06	5%

Table 4-10 *– Relationship Between Compressive Strength and Young's Modulus*

As seen from the table, the ACI equation provides conservative values compared to that of the Static Modulus tests. The equation using the density of the concrete (**Equation 4-10**) yielded values much less than the Static Young's Modulus values at earlier ages. The error % decreases with age. This is because the ACI equations are designed for f'_c which is the compressive strength at 28 days. The equations were not as conservative for the SCC batch, but still resulted in lower modulus values compared to the actual Static Modulus.

Chapter 5 Conclusions and Recommendations

5.1 – Relationship Between Static and Dynamic Modulus of Elasticity

The Dynamic Modulus of Elasticity obtained from Ultrasonic Pulse Wave Velocities was determined to be approximately 16% greater than the determined Static Modulus of Elasticity at any age for each of the different concrete mixes. The UPV method also resulted in higher modulus values than those determined from the vibration resonance method by approximately 10%. Concrete contains voids and free water that the pulse waves must propagate through, but would not be detectable by the vibration impact because of the much larger wave length. This is the basis for the difference between E_{UPV} and E_{Impact}. The results obtained from this research project proved to be in accordance with literature review.

It was also proven that there were clear linear relationships between E and E_{UPV}, as well as E and E_{Impact}. It was determined that there was a strong linear relationship between the modulus values obtained from the two dynamic testing methods, E_{UPV} and E_{Impact} as well. As discussed earlier, unlike the Static test, dynamic tests only apply a small amount of force to the specimens, and therefore do not cause any deformations of the specimen during the testing phase. This could be the reason why the Dynamic Modulus often proves to be higher than the Static Modulus, as proven through this research project. The composite nature of concrete is also a basis for the difference in moduli values. Homogenous materials such as steel and paste specimens do not exhibit this behavior. Concrete is comprised of aggregates and sand particles which greatly alter its homogeneity.

The Dynamic and Static Modulus values also seemed to converge at later ages. This could be due to the increase of degree of hydration in the concrete at later ages. At early ages, concrete has a low degree of hydration, and the free water in concrete would have a greater effect on the Static Modulus testing. This could result in a greater separation between these values at early ages. As concrete matures, the degree of hydration increases, and axial static loading will not deform the specimen as much. This would cause the two modulus values to converge at later ages.

The resonance vibration resonance technique provided results closest to the Static Modulus (5% difference), and therefore proves to be the most accurate and feasible means of determining the Young's Modulus of concrete through dynamic testing methods.

5.2.1 – Additional Research

For this research study, only four different concrete mixes were tested. Additional concrete mixes, and an overall larger sample size should be studied to acquire more accurate results. Due to time constraints, the specimens were only studied up until 28-days. Specimens should be tested at much longer lengths of time to determine if the relationships between moduli values remains constant, or if they continue to converge even more at later ages.

5.2 – Relationship Between Compressive Strength and Young's Modulus

As seen in the previous section, the ACI equation used to estimate Young's Modulus resulted in conservative values when compared to the actual modulus obtained from the Static Loading Test. In most cases, the modulus values estimated from the 28-day compressive strength was about 20% lower than the actual Static Modulus. The ACI equation resulted in

closer values for the SCC batch (approximately 5% lower than the actual Static Modulus). This could be because the equations were designed for normal-strength concrete, and as seen in the compressive strength, SCC is high-strength. Although it is better for these values to be conservative as opposed to greater than the calculated Static Modulus, there can be costly ramifications for over-strengthening the concrete. There have been many research studies conducted to try and develop more accurate equations to estimate Young's Modulus. The problem with these empirical relationships, is that in most cases, they can only be applicable to certain types of concrete mixes. More studies need to be conducted in the future to enhance the accuracy of these relationships.

References

Aggarwal, P., Siddique, R., Aggarwal, Y., and M Gupta, S. (2008). *Self-Compacting Concrete-Procedure for Mix Design*. Leonardo Electronic Journal of Practices and Technologies.

ASTM C39 / C39M-16b, Standard Test Method for Compressive Strength of Cylindrical Concrete Specimens, ASTM International, West Conshohocken, PA, 2016, www.astm.org

ASTM C192 / C192M-16a, Standard Practice for Making and Curing Concrete Test Specimens in the Laboratory, ASTM International, West Conshohocken, PA, 2016, www.astm.org

ASTM C215-14, Standard Test Method for Fundamental Transverse, Longitudinal, and Torsional Resonant Frequencies of Concrete Specimens, ASTM International, West Conshohocken, PA, 2014, www.astm.org

ASTM C231 / C231M-14, Standard Test Method for Air Content of Freshly Mixed Concrete by the Pressure Method, ASTM International, West Conshohocken, PA, 2014, www.astm.org

ASTM C469 / C469M-14, Standard Test Method for Static Modulus of Elasticity and Poisson's Ratio of Concrete in Compression, ASTM International, West Conshohocken, PA, 2014, www.astm.org

ASTM C496 / C496M-11, Standard Test Method for Splitting Tensile Strength of Cylindrical Concrete Specimens, ASTM International, West Conshohocken, PA, 2004, www.astm.org

ASTM C597-16, Standard Test Method for Pulse Velocity Through Concrete, ASTM International, West Conshohocken, PA, 2016, www.astm.org

ASTM C1611 / C1611M-14, Standard Test Method for Slump Flow of Self-Consolidating Concrete, ASTM International, West Conshohocken, PA, 2014, www.astm.org

ASTM C1621 / C1621M-14, Standard Test Method for Passing Ability of Self-Consolidating Concrete by J-Ring, ASTM International, West Conshohocken, PA, 2014, www.astm.org

Azamirad, H. and Beheshti zadeh, D. (2005). *A Criticism of Self Compacting Concrete.* Singapore Concrete Institute.

Benefits & Advantages of Self Compacting Concrete. (n.d.) Retrieved from: http://theconstructor.org/concrete/benefits-advantages-of-self-compacting-concrete/7683/

Bouzaoubaa, N., Foo, S. (2005). *Use of Fly Ash and Slag in Concrete: A Best Practice Guide.* Materials Technology Laboratory.

Chapman & Hall. *Testing of Concrete in Structures.* (1996).

Chavhan, P. and Vyawahare, M. (2015). *Correlation of Static and Dynamic modulus of Elasticity for Different SCC Mixes.* International Journal on Recent and Innovation Trends in Computing and Communication.

Daczko, J. (2012). *Self Consolidating Concrete*. Spon Press.

Dashti, D. (2016). *A Study of NDT Techniques Using Ultrasonic Pulse Velocity Test and Microwave Oven Method on SCC and TVC.*

De Schutter, G. (2005). *Guidelines for Testing Fresh Self-Compacting Concrete*. Testing-SCC.

European Federation of Concrete Admixture Associations (2006). *Guidelines for Viscosity Modifying Admixtures for Concrete.* EFNARC.

Germann Instruments. (n.d.) *Pundit.*

Grosse, C. U., & Reinhardt, H. W. (1996). *The Resonance Method - Application of a New Nondestructive Technique Which Enables Thickness Measurements at Remote Concrete Parts*. NDTnet, 1(10).

Gudmarsson, A. (2014). *Resonance Testing of Asphalt Concrete.*

Gurjar, A. (2004). *Mix Design and Testing of Self-Consolidating Concrete Using Florida Materials.* Florida Department of Transportation.

Halabe et al. (1995). *Nondestructive Evaluation Methods for Highway Bridge Superstructures.*

Hershberger, J. (2015). *A Study of Self Consolidating Concrete for Cast in Place Applications: Current Practices, Rapid W/CM Determination, and Stability Effects of Pumping.*

Hime, W. (1994). *Analyses for Cement and Other Materials in Hardened Concrete*. Significance of Tests and Properties of Concrete and Concrete-Making Materials.

International Atomic Energy Agency. (2002). *Guidebook on Non-Destructive Testing of Concrete Structures.*

Lee, K., Kim, D., and Kim, J. (1997). *Determination of dynamic Young's modulus of concrete at early ages by impact resonance test.* KSCE Journal of Civil Engineering.

Khayat, K. and Schutter, G. (2014). *Mechanical Properties of Self-Compacting Concrete.* Springer.

Khayat, K. (1999). *Workability, Testing, and Performance of Self-Consolidating Concrete.* Aci Materials Journal.

Koehler, E. (2007*). Aggregates in Self-Consolidating Concrete.*

Koehler, E. (2007). *Self-Consolidating Concrete for Precast Structural Applications: Mixture Proportions, Workability, and Early-Age Hardened Properties.* CTR.

Kumar, D. and Rajeev, C. (2012). *Development of Self Compacting Concrete by use of Portland Pozzolana Cement, Hydrated Lime and Silica Fume.* ISCA Journal of Engineering Sciences.

Lorenzi, A., Tisbierek, F., Filjo, L. *Ultrasonic Pulse Velocity Analysis in Concrete Specimens.* AAENDE.

Murthy.N, K., Rao A.V., N., Reddy I. Vand, R., and Reddy.M, V. (2012). *Mix Design Procedure for Self Compacting Concrete.* IOSR Journal of Engineering.

Okamura, H., Ouchia, M. (2003). *Self-Compacting Concrete.* Journal of Advanced Concrete Testing.

Olafusi, O., Adewuyi, A., Otunla, A., and Babalola, A. (2015). *Evaluation of Fresh and Hardened Properties of Self-Compacting Concrete.* Open Journal of Civil Engineering.

Parra, C., Valcuende, M., and Gomez, F. (2010). *Splitting Tensile Strength and Modulus of Elasticity of Self-Compacting Concrete.* Construction and Building Materials.

Pickett, G. (1945). "Equations for Computing Constants From Flexural and Torsional Resonant Frequencies of Vibration of Prisms and Cylinders." *Proceedings of the American Society for Testing and Materials,* vol 45, pp. 846-846.

Popovics, J. (2008). *A Study of Static and Dynamic Modulus of Elasticity of Concrete.* American Concrete Institute - Concrete Research Council, Urbana, IL.

Poulson, B. (2002). *Specification and Guidelines for Self-Compacting Concrete.* EFNARC.

Plachy, T., Padevet, P., and Polak, M. (n.d.). *Comparison of Two Experimental Techniques for Determination of Young's Modulus of Concrete Specimens.* Recent Advances in Applied and Theoretical Mechanics.

Salman, M. and Al-Amawee, A. (2006). *The Ratio between Static and Dynamic Modulus of Elasticity in Normal and High Strength Concrete.* Journal of Engineering and Development.

Self Compacting Concrete. (2010.) Retrieved from: http://civil-resources.blogspot.com/2010/06/self-compacting-concrete.html

Stunba, I., Tmik, A. (2006). *Correction Coefficients for Calculating the Young's Modulus from the Resonant Flexural Vibration.* Journal of Mechanical Engineering, vol 52, pp. 317-322.

Subramaniam, K., Popovics, J., and Shah, S. (2000). *Determining Elastic Properties of Concrete Using Vibrational Resonance Frequencies of Standard Test Cylinders.* Cement Concrete and Aggregates.

Sweet, J., Chen, R. (2012) *Implementation of self-consolidating concrete in caisson construction for the Stalnaker Run Bridge.* Construction and Building Materials, vol 34, pp. 545-553.

Therian, M. (2008). *Experimental Evaluation of the Modulus of Elasticity of Self-Consolidating Concrete.*

Thomas, M. (2007). *Optimizing the Use of Fly Ash in Concrete.* Portland Cement Association.

Trtnik, G., Kavcic, F., Goran, T. (2007). *Prediction of Concrete Strength Using Ultrasonic Pulse Velocity and Artificial Neural Networks.* Elsevier.

Umar, A., Al-Taminmi, A. (2011). *Influence of Viscosity Modifying Admixture (VMA) on the Properties of SCC Produced Using Locally Supplied Materials in Bahrain.* Jordan Journal of Civil Engineering.

V Funnel Test on Self Compacting Concrete. (n.d.) Retrieved from: http://theconstructor.org/practical-guide/v-funnel-test-on-self-compacting-concrete/6034/

Vachon, M. (2002). *ASTM Puts Self-Consolidating Concrete to the Test*. Standardization News.

Vaclavik, V., Dirner, V., Dvorsky, T., Daxner, J. (2012). *The Use of Blast Furnace Slag.*

Yaman, I., Inci, G., Yesiller, N., Aktan, H. (2001). *Ultrasonic Pulse Velocity in Concrete Using Direct and Indirect Transmission.* ACI Materials Journal.

VITA

Logan Trifone was born in Hollywood, MD on March 10, 1993. After graduating high school in 2011, he began pursuing a degree in Civil Engineering from West Virginia University. Upon receiving a B.S. in Civil Engineering in the spring of 2015, he began graduate school at the College of Engineering at West Virginia University. He will graduate in May of 2017 with a Master's of Science in Civil Engineering specializing in Structural Engineering.